ANNUAL REVIEWS Further
Click here to view this article's online features:
- Download figures as PPT slides
- Navigate linked references
- Download citations
- Explore related articles
- Search keywords

Fukushima Daiichi–Derived Radionuclides in the Ocean: Transport, Fate, and Impacts

Ken Buesseler,[1] Minhan Dai,[2] Michio Aoyama,[3] Claudia Benitez-Nelson,[4] Sabine Charmasson,[5] Kathryn Higley,[6] Vladimir Maderich,[7] Pere Masqué,[8,9] Paul J. Morris,[10] Deborah Oughton,[11] and John N. Smith[12]

[1]Woods Hole Oceanographic Institution, Woods Hole, Massachusetts 02543; email: kbuesseler@whoi.edu*

Annu. Rev. Mar. Sci. 2017. 9:173–203

First published online as a Review in Advance on June 30, 2016

The *Annual Review of Marine Science* is online at marine.annualreviews.org

This article's doi: 10.1146/annurev-marine-010816-060733

Copyright © 2017 Ken Buesseler et al. This work is licensed under a Creative Commons Attribution 4.0 International License, which permits unrestricted use, distribution, and reproduction in any medium, provided the original author and source are credited. See credit lines of images or other third party material in this article for license information.

*Author affiliations for all coauthors can be found in the Acknowledgments section.

Keywords

cesium, caesium, North Pacific, radioactivity, Japan

Abstract

The events that followed the Tohoku earthquake and tsunami on March 11, 2011, included the loss of power and overheating at the Fukushima Daiichi nuclear power plants, which led to extensive releases of radioactive gases, volatiles, and liquids, particularly to the coastal ocean. The fate of these radionuclides depends in large part on their oceanic geochemistry, physical processes, and biological uptake. Whereas radioactivity on land can be resampled and its distribution mapped, releases to the marine environment are harder to characterize owing to variability in ocean currents and the general challenges of sampling at sea. Five years later, it is appropriate to review what happened in terms of the sources, transport, and fate of these radionuclides in the ocean. In addition to the oceanic behavior of these contaminants, this review considers the potential health effects and societal impacts.

OPEN ACCESS CC BY

1. INTRODUCTION

On March 11, 2011, the Tohoku earthquake and resulting tsunami led to an unprecedented release of artificial radionuclides to the ocean from the Fukushima Daiichi nuclear power plants (FDNPPs). Whereas immediate health concerns often focus on short-lived radioactive contaminants, environmental impacts center on the longer-lived radionuclides (half-lives of more than 1 year). Unlike the Chernobyl nuclear power plant (CNPP) (Ukraine) accident that occurred 25 years earlier and breached the core of the reactor, the FDNPP releases were considerably smaller and comprised more-volatile radionuclides and gases, such as the radioisotopes ^{134}Cs (half-life of 2.06 years) and ^{137}Cs (half-life of 30.2 years). The magnitude of the total release of ^{137}Cs from the FDNPPs (detailed below) is approximately 50 times smaller than that of global fallout from atmospheric nuclear weapons testing (which peaked in the early 1960s) and approximately 5 times smaller than that of the CNPP accident, and is similar to that resulting from intentional discharges from the Sellafield nuclear fuel reprocessing plant (Cumbria, England) (Buesseler 2014).

This review presents the current state of knowledge regarding artificial radionuclides released to the ocean from the FDNPPs. Although the focus is on radioisotopes of Cs, we discuss other artificial radionuclide contaminants when appropriate. We begin with a summary of inputs to the ocean, including atmospheric fallout, direct discharge, and land-derived sources of FDNPP radionuclides. We also examine the transport and fate of Cs, starting with its transport and mixing via physical processes such as ocean currents, and then discuss its far less dominant but important association with detrital and biogenic particles and their transport to, and fate on, the seafloor. The biological uptake of FDNPP contaminants and their possible dose effects on marine biota are also addressed. We conclude with a discussion of human health and societal concerns.

Throughout the discussion, we report radionuclide activities in units of becquerels (1 Bq = one disintegration event per second), most often per cubic meter for seawater or per kilogram when discussing sediments and biota. Total inventories are generally presented in units of PBq (10^{15} Bq), with TBq (10^{12} Bq) and GBq (10^{9} Bq) used when discussing smaller inventories and fluxes. If not otherwise specified, all data are decay corrected to the time of sampling.

2. SOURCES OF FUKUSHIMA DAIICHI–DERIVED RADIONUCLIDES TO THE OCEAN

There are four major sources of FDNPP-derived radionuclides to the environment (**Figure 1**). The largest and earliest source was the initial venting and explosive releases of gases and volatile radionuclides to the atmosphere, which led to fallout on both land and the ocean. Atmospheric fallout peaked around March 15 (Chino et al. 2011, Morino et al. 2011, Huh et al. 2012, Stohl et al. 2012); transport models suggested that more than 80% of the fallout was on the ocean surface, with the highest deposition in coastal waters near the FDNPPs, although there are no atmospheric fallout data over the ocean to measure this directly. Subsequent to the atmospheric fallout was the somewhat smaller direct discharge of contaminated material to the ocean during emergency cooling efforts at the FDNPPs that resulted in runoff over land, enhanced flow of contaminated groundwater, and stagnant water leakage from the basement of the reactor buildings into the ocean. This secondary release process peaked around April 6, 2011, when the highest FDNPP-derived radiocesium activities were observed in the ocean in close proximity to the FDNPPs (e.g., Buesseler et al. 2011).

Ongoing radionuclide releases to the ocean from land through rivers, runoff, and groundwater flow must also be considered. These sources are influenced by an array of complex processes, but they are much smaller than the initial atmospheric fallout and subsequent direct discharges.

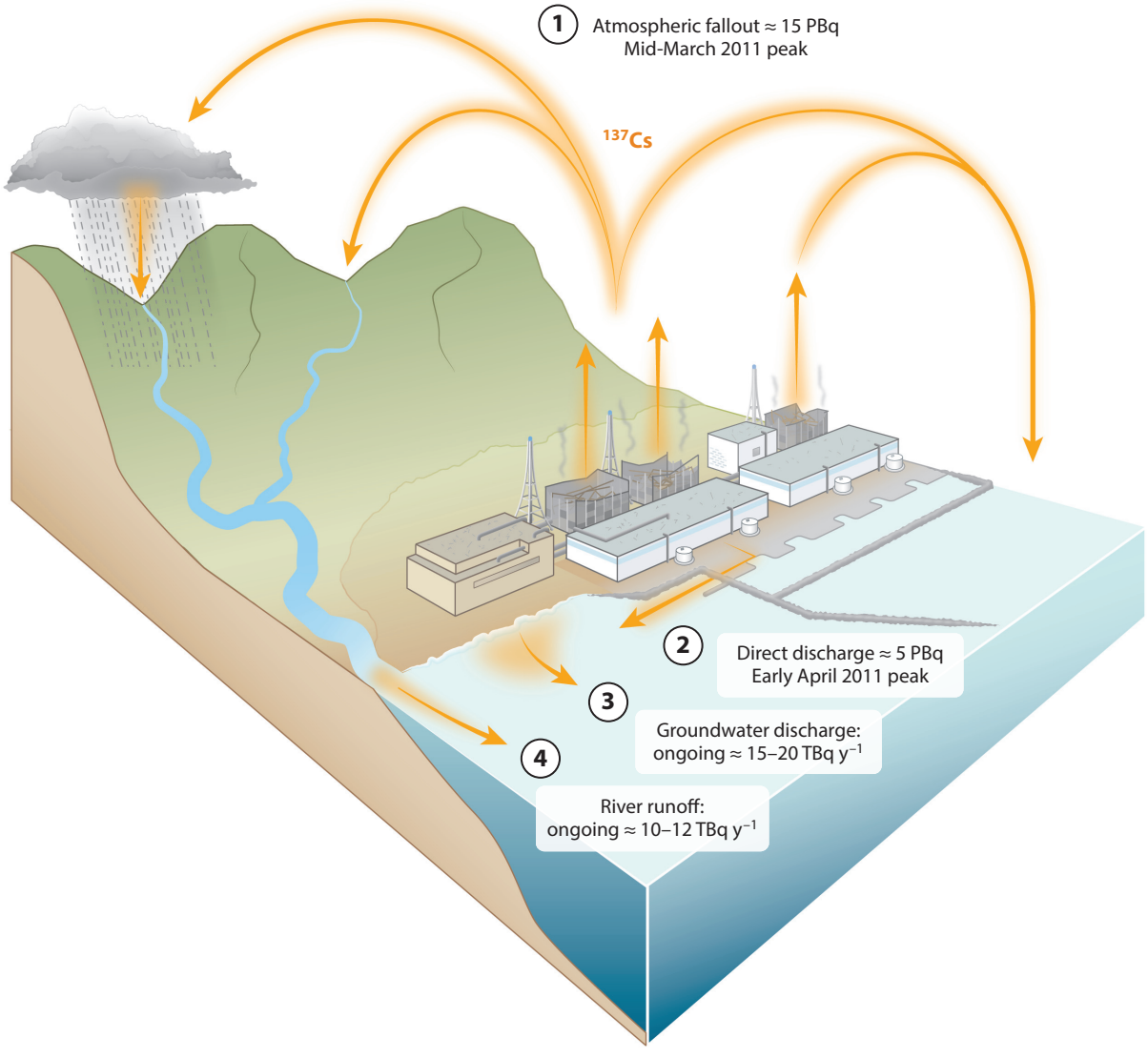


Figure 1

Schematic of Fukushima Daiichi–derived sources of ^{137}Cs. Atmospheric fallout (①) and direct discharge (②) are shown as total petabecquerels (PBq) released in the first month of the accident (median values from **Table 1**). Groundwater fluxes (③) and river runoff (④) are approximate ranges for the first year in terabecquerels (TBq), a unit 1,000 times smaller than the PBq used for fallout and direct discharge.

In the following discussion, it should be noted that ^{137}Cs levels in the Pacific are governed by a combination of background fallout and FDNPP contamination, whereas ^{134}Cs levels are associated entirely with FDNPP inputs, because the background fallout of this shorter-lived radionuclide has decayed almost completely in the modern day. During the first month after the FDNPP releases, measured ^{134}Cs/^{137}Cs activity ratios in reactor discharges were uniform and very close to unity (0.99 ± 0.03) (Buesseler et al. 2011). Therefore, when ^{134}Cs activity levels are decay corrected

Table 1 Source estimates for ^{137}Cs from the Fukushima Daiichi nuclear power plants

Reference	Total atmospheric fallout (PBq)	Atmospheric fallout on ocean (PBq)	Direct discharge to ocean (PBq)	Total in North Pacific (PBq)
Chino et al. 2011	13			
Katata et al. 2012	11			
Mathieu et al. 2012	20.6			
Stohl et al. 2012	36 (23–50)			
Terada et al. 2012	8.8			
Kobayashi et al. 2013	13	7.6	3.5	
Saunier et al. 2013	15.5			
Winiarek et al. 2014	19.3			
Katata et al. 2015	14.5			
Kawamura et al. 2011		5	4	
Bailly du Bois et al. 2012		11.5	27 ± 15	
Estournel et al. 2012		5.8 ± 0.1	4.3 ± 0.2	
Tsumune et al. 2012, 2013			3.5 ± 0.7	
Charette et al. 2013			13.5 ± 2.5	
Miyazawa et al. 2013			5.6 ± 0.2	
Rypina et al. 2013			16.2 ± 1.6	
Aoyama et al. 2016	15.2–20.4	11.7–14.8		15.2–18.3
Inomata et al. 2016				15.3 ± 2.6
Tsubono et al. 2016		10.5 ± 0.9		16.1 ± 1.4

to the time of initial release, they reflect the activity levels of ^{137}Cs specifically derived from the FDNPPs. As a consequence, measurements of ^{134}Cs can be used as a proxy to resolve ^{137}Cs inventories into the components derived separately from background fallout and the FDNPPs, which simplifies calculations of total discharges from the FDNPPs. Here, we provide different estimates of each of the source terms for radiocesium and include a brief comparison with four other radionuclides: ^{90}Sr, Pu, ^{129}I, and ^{131}I.

Estimates of the total atmospheric fallout of **^{137}Cs** vary greatly because of the uncertainty in the transport and deposition parameters in the atmospheric models as well as the lack of observations required to conduct inverse calculations (**Table 1**). Some of these studies constrained their atmospheric deposition models using terrestrial and/or surface ocean observations, and these estimates ranged from 8.8 to 50 PBq (Katata et al. 2012, Mathieu et al. 2012, Stohl et al. 2012, Terada et al. 2012, Kobayashi et al. 2013, Saunier et al. 2013, Winiarek et al. 2014, Katata et al. 2015). Other studies estimated atmospheric fallout deposition over the ocean only, and these estimates ranged from 5 to 14.8 PBq (Kawamura et al. 2011, Estournel et al. 2012, Kobayashi et al. 2013, Aoyama et al. 2016).

To constrain the total direct discharge of radiocesium released to the oceans, several groups have used ocean models combined with observations of Cs in surface water close to the FDNPPs during the period of highest direct discharge, from March to May 2011 (Kawamura et al. 2011, Estournel et al. 2012, Kobayashi et al. 2013, Miyazawa et al. 2013). Tsumune et al. (2012, 2013) were also able to use the ^{131}I/^{137}Cs activity ratio to further distinguish periods of direct discharge and atmospheric inputs; their estimates of direct discharge averaged 3.5 ± 0.7 PBq (**Table 1**).

Somewhat higher estimates of direct discharge are derived from three studies using ocean models and observations made after May 2011 and/or over longer time periods. Bailly du Bois et al. (2012) estimated the direct discharge of ^{137}Cs using an interpolation of observations collected from April 11 to July 11, 2011. Over the course of their observations, they documented a 50% decrease in surface ocean ^{137}Cs every 7 days. Using this rate and extrapolating back to the peak in ^{137}Cs in early April, they estimated a total direct discharge of 27 $\pm$ 15 PBq. Charette et al. (2013) combined independent assessments of the average water mass age using radium isotopes during June 4–18, 2011. Using a mixing/dilution model and the assumption that the mixing regime was constant, they predicted a direct discharge of 13.5 $\pm$ 2.5 PBq. Rypina et al. (2013) used ^{137}Cs data from the same cruise and numerical simulations to determine that more than 95% of the ^{137}Cs remaining in the study area within 600 km off Japan was due to direct discharge, because the earlier fallout Cs would have already been transported farther offshore. The strength of the direct discharge source needed to account for their observations was 16.2 $\pm$ 1.6 PBq.

A final set of source estimates was derived using a detailed tally of field-based Cs inventories across the North Pacific and thus includes both atmospheric and direct discharge sources. Aoyama et al. (2016) estimated a North Pacific ^{137}Cs inventory of 15.2–18.3 PBq. This group calculated the inventories using a standard mixed layer of 50 m over 10° $\times$ 10° areas between 20°N and 50°N, relying on ships of opportunity to extend surface sampling across the Pacific in April and May 2011. Their inventory is in close agreement with two recent estimates, of 15.3 $\pm$ 2.6 PBq by Inomata et al. (2016) and 16.1 $\pm$ 1.4 PBq by Tsubono et al. (2016), which used more comprehensive ocean data sets and interpolation methods and models.

All of these estimates are limited by the shortage of vertical concentration profiles and spatial coverage, especially for locations farther offshore than those regularly monitored by Japanese agencies near the FDNPPs. Several of the estimates above are acknowledged to likely be underestimates owing to the lack of sampling in some regions. Nonetheless, estimates tend to converge to between 15 and 20 PBq for the combined FDNPP inputs of ^{137}Cs from atmospheric fallout and direct discharge to the North Pacific. This represents an additional input of approximately 25% more ^{137}Cs than existed in the North Pacific prior to the FDNPP event (69 PBq) from nuclear weapons testing (Aoyama et al. 2016). Adding an equal amount of ^{134}Cs would double the radiocesium inventory derived from the FDNPPs in 2011.

Radiocesium inputs to Japanese coastal waters also occur via riverine sources and surface water runoff (Chartin et al. 2013, Nagao et al. 2013, Evrard et al. 2015). Cs has a high affinity for particles in freshwater, and thus its transport and delivery via rivers are associated largely with high sediment loads that occur during heavy rains and flood events. For example, Nagao et al. (2013) found that as much as half of the annual Japanese ^{137}Cs river flux to the coastal ocean occurred during heavy precipitation. Yamashiki et al. (2014) found that suspended particle loads from the Abukuma River basin delivered 5 TBq of ^{137}Cs (1 TBq $= 10^{-3}$ PBq) to the northern coastal zone in a 10-month period, with more than half of the delivery occurring during a single typhoon that remobilized sediments during an 8-day period.

In a review of Cs transfer from land to the ocean, Evrard et al. (2015) summarized modeling simulations indicating that up to 10–12 TBq of particle-associated ^{137}Cs was transferred from land to the ocean after the initial release, specifically during the first year. This would correspond to less than 1–2% of the total inventory deposited on land. Models suggest that up to 155 TBq of ^{137}Cs will continue to be exported to the ocean over the next century (Pratama et al. 2015). Once in the ocean, particulate Cs remains largely irreversibly bound, with experiments showing only a few percent desorption from soil in seawater (Yamashiki et al. 2014).

Submarine groundwater discharge represents an additional long-term source of radiocesium to the ocean, in particular from the contaminated FDNPP site. Kanda (2013) used the exchange rate of water in the harbor at the FDNPP site and differences in seawater Cs concentrations inside and outside the harbor to calculate an average release rate of 93 GBq d^{-1} for the summer of 2011 and 8 GBq d^{-1} in the summer of 2012 (1 GBq $= 10^{-6}$ PBq). From July 2012 until March 2015, ^{137}Cs activity in the surface water near the FDNPP site decreased from approximately 10,000 to 1,000 Bq m^{-3}, and studies have calculated a discharge rate of approximately 30 GBq d^{-1} in 2013 and 10 GBq d^{-1} in 2014 (Tsumune et al. 2013, Aoyama et al. 2016). These rates are small relative to those for the first month after the initial release, when ^{137}Cs inputs were five to six orders of magnitude higher (15–20 PBq in 30 days $= 0.5–0.7 \times 10^6$ GBq d^{-1}). Note that the magnitudes of the river inputs discussed above are similar to those for the continuing input sources via groundwater at the FDNPPs, although (as discussed above) most of the river input to the ocean consists of particle-associated Cs, whereas inputs of dissolved Cs are dominant in groundwater.

In terms of other radionuclides of the greatest health concern with half-lives of more than 1 year, ^{90}Sr, ^{239,240}Pu, and ^{129}I are of the most interest here. Levels of ^{90}Sr from the FDNPPs in atmospheric fallout were, at most, four orders of magnitude lower than ^{137}Cs measured on land owing to its low volatility (Povinec et al. 2012, Steinhauser et al. 2014, Tanaka et al. 2014). Most of the ^{90}Sr released from the FDNPPs was directly discharged to the North Pacific, with estimates of total inventories ranging from 0.04 to 1.0 PBq (Casacuberta et al. 2013, Povinec et al. 2012).

Since the initial discharges, there have been reported spills of liquid radioactive waste at the FDNPP site and corresponding anomalies in the ^{90}Sr activities in seawater, with ^{90}Sr activities exceeding those of ^{137}Cs in the ocean near the FDNPP site for short periods of time (Povinec et al. 2012, Castrillejo et al. 2015). An initial ^{137}Cs/^{90}Sr ratio of 39 ± 1 in seawater was measured 30–600 km seaward of the FDNPPs in June 2011, which is significantly higher than the global atmospheric fallout ratio of 1.6 but closer to the ^{137}Cs/^{90}Sr ratio of 12.5 measured in stagnant water at the FDNPP site (average core release ratio from Nishihara et al. 2012). ^{137}Cs/^{90}Sr ratios decreased with time, averaging 3.8 in 2013 in waters within 100 km of the FDNPP site (Castrillejo et al. 2015). Because the ^{90}Sr half-life (29 years) is close to that of ^{137}Cs, this decrease is not related to radioactive decay. Rather, it is hypothesized to be a result of continuing accidental spills and/or the higher mobility of Sr, as Cs is more strongly adsorbed onto soil particles, whereas Sr remains largely dissolved and thus relatively enriched in any ongoing releases via groundwater.

Castrillejo et al. (2015) used data on ^{134}Cs concentrations and the distinct relationship between ^{90}Sr and ^{137}Cs to estimate that the FDNPPs leaked ^{90}Sr into the North Pacific at a rate of 2.3–8.5 GBq d^{-1} in September 2013. This confirms the Tokyo Electric Power Company (TEPCO) monitoring data through June 2015, which showed activities of ^{90}Sr and ^{137}Cs up to 10 and 1,000 times higher, respectively, than pre-March 2011 concentrations near the discharge channels of the FDNPPs.

In addition to ^{90}Sr, the potential release of long-lived Pu isotopes is of considerable public concern because these isotopes present a potentially large health risk for internal radiation exposure. Zheng et al. (2013) summarized studies related to the release of Pu from the FDNPPs. Ratios of FDNPP-derived ^{137}Cs to ^{239,240}Pu are 1 million or greater, based on an examination of leaf litter and soils in which isotopic ratios of Pu were used to distinguish weapons-testing-derived Pu from FDNPP-derived Pu (Zheng et al. 2012, Evrard et al. 2015). In total, only a relatively small amount of Pu, on the order of $1.0–2.4 \times 10^9$ Bq of ^{239,240}Pu, was released into the environment from the damaged FDNPP reactors (Zheng et al. 2012). This is consistent with the low volatility of this radionuclide and the limited explosive releases from the FDNPPs, in contrast to the CNPP, where as much as 3×10^{13} Bq of ^{239,240}Pu was released (Steinhauser et al. 2014).

Several ocean studies off the Japanese coast have not been able to detect Pu contamination from the FDNPPs (e.g., Bu et al. 2013). In addition, Pu from the FDNPPs was not detected in the marginal seas of the Pacific, such as the South China Sea (Wu et al. 2014). The challenge in these studies, as on land, is in separating the weapons-testing component of Pu that was already present in the environment from an even smaller additional component of FDNPP Pu.

Approximately 1 kg of the long-lived ^{129}I (half-life of 16 million years) was also released from the FDNPPs, mainly through direct discharges into the ocean (Guilderson et al. 2014). These discharges resulted in only small incremental increases in seawater concentrations of ^{129}I in excess of fallout levels in the upper 250 m of the water column proximal to the FDNPPs. Owing to its long half-life, however, ^{129}I may be useful as an ocean circulation tracer of the FDNPP releases in future years.

Finally, although ^{131}I has a short half-life (8 days), it is of significant health concern on land, though less so in the ocean. Its distribution generally followed that of ^{137}Cs, but with a more rapid decrease in concentration with time because of radioactive decay. Observations suggest that the ^{131}I/^{137}Cs ratio was more variable in atmospheric fallout to the ocean prior to March 26, 2011, and more constant thereafter (corrected for decay). This change in variability has been used to argue that the dominant source of radiocesium to the coastal ocean was initially atmospheric fallout but changed to direct discharge thereafter (e.g., Chino et al. 2011, Inomata et al. 2016).

A discussion of other less abundant radionuclides is beyond the scope of this review. Several studies have reported on them and compared their relative contributions from the FDNPPs and earlier sources (e.g., Steinhauser 2014, Steinhauser et al. 2014).

3. CESIUM OCEAN DISTRIBUTIONS AND TRANSPORT ACROSS THE NORTH PACIFIC

Prior to 2011, the ^{137}Cs activity in surface water of the North Pacific and its marginal seas was 1–2 Bq m^{-3} as a consequence of atmospheric nuclear weapons testing (Aoyama et al. 2008, 2011). In March 2011, ^{137}Cs levels increased rapidly, to as much as 68 million Bq m^{-3} by early April, in surface waters directly adjacent to the FDNPP site, and then decreased by more than three orders of magnitude within about a month, to approximately 10,000 Bq m^{-3} through early 2012 (Buesseler et al. 2011), and to approximately 1,000 Bq m^{-3} from 2013 to 2015 (the discussion of marine biota below also addresses seawater time history). Time-series measurements after March 2011 from research cruises, ships of opportunity, and contributions from citizen scientists sampling the west coast of North America have provided a growing number of FDNPP-related data that are being collated by the International Atomic Energy Agency (IAEA 2015b).

Given that Cs is extremely soluble, with less than 1% of ^{137}Cs and ^{134}Cs found on marine particles in the open ocean (Aoyama & Hirose 1995), its subsequent dispersion in the marine environment is controlled mainly by physical ocean processes, at least on decadal timescales (see discussion below of sediment traps and Cs residence time). Therefore, Cs from both atmospheric fallout and direct discharge is expected to follow oceanic transport and mixing pathways. Note, however, that a small fraction of the fallout was transported by atmospheric winds more rapidly across the North Pacific and the rest of the globe, resulting in low but detectable activities of FDNPP Cs in some distant oceanic regions and at many atmospheric sampling stations far removed from Japan (Masson et al. 2011, Inoue et al. 2012, Lujanienė et al. 2012, Min et al. 2013, Evangeliou et al. 2014, Kaeriyama et al. 2014, Kumamoto et al. 2014).

The majority of the FDNPP-derived radionuclides were mixed and diluted quite rapidly in the energetic coastal waters off Japan under the influence of currents, tidal forces, and eddies, with the major flow of the contaminated plume moving eastward under the influence of the

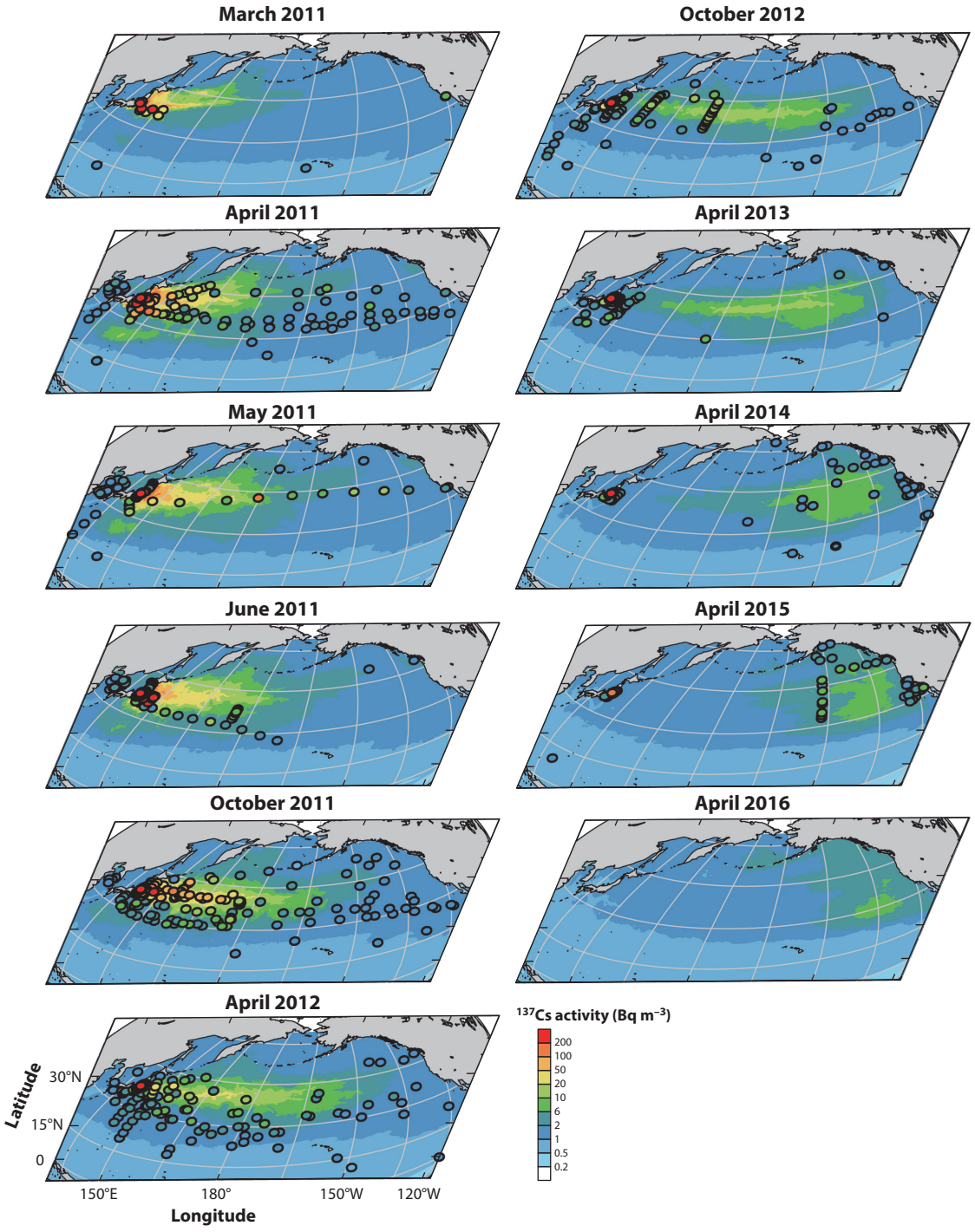
southward-flowing Oyashio Current and the stronger, northward- and eastward-flowing Kuroshio Current (**Figure 2**). The southward transport of the plume, or at least its surface expression, was blocked by the Kuroshio Current, which formed a boundary between FDNPP-affected surface waters to the north and unaffected waters in the core of the current and to the south (Buesseler et al. 2012). The eastward progression of the FDNPP plume was driven by the North Pacific Current, which bifurcates as it approaches North America, diverging into the northward-flowing Alaska Current and the southward-flowing California Current. The movement of the leading edge of the plume indicates an average speed of propagation of 7 km d^{-1} (8 cm s^{-1}) until March 2012 and 3 km d^{-1} (3.5 cm s^{-1}) from March 2012 through August 2014 (Aoyama et al. 2016). These results are consistent with a drifter-based estimate of the horizontal spread of the FDNPP plume (Rypina et al. 2014).

The arrival of FDNPP-derived radionuclides off the west coast of North America was documented by measurements of ^{134}Cs and ^{137}Cs on the Canadian continental shelf in June 2013 (Smith et al. 2015). By February 2014, the ^{137}Cs signal had increased to 2 Bq m^{-3} throughout the upper 150 m, doubling the signal associated with fallout background from atmospheric nuclear weapons tests (Smith et al. 2015). These activities have continued to increase over time, with offshore ^{137}Cs values in the eastern North Pacific approaching 6 Bq m^{-3} in 2014 and 10 Bq m^{-3} in 2015, approximately 2,000 km north of Hawaii. The first arrival of FDNPP Cs on the shoreline of North America was detected in February 2015 in British Columbia by citizen scientists and was distinguished by ^{137}Cs and ^{134}Cs activities of 5.6 Bq m^{-3} and 1.4 Bq m^{-3}, respectively (6.1 Bq m^{-3} for ^{137}Cs and 5.0 Bq m^{-3} for ^{134}Cs when decay corrected to a 2011 release date; hence, the difference of 1.1 was background ^{137}Cs at this site prior to the initial FDNPP releases). By 2015, FDNPP radiocesium had been detected as far north as 55°N and as far south as approximately 25°N at activities marginally above the fallout background (data from **http://ourradioactiveocean.org/results** and **http://fukushimainform.ca/archived-monitoring-results**).

Throughout much of the Pacific Ocean, the FDNPP plume was rapidly mixed throughout the upper 100–150 m of the water column and has only more slowly begun to penetrate to intermediate water depths (Buesseler et al. 2012, Smith et al. 2015, Yoshida et al. 2015). An important exception is the subsurface transport of FDNPP Cs in various Pacific mode waters that are formed through winter cooling and buoyancy loss, leading to mixing and homogenization of hydrographic properties deep in the water column (Aoyama et al. 2016). In June 2012, the ^{134}Cs activity reached a maximum of 6.1 $\pm$ 0.5 Bq m^{-3} at approximately 150 m at 29°N, 165°E. This subsurface maximum, which was also observed along 149°E, likely reflects the southward transport of FDNPP-derived radiocesium in association with the formation and subduction of the Subtropical Mode Water. In June 2012 at 34–39°N along 165°E, the ^{134}Cs activity exhibited a maximum at approximately 350 m, which corresponds to the Central Mode Water. These observations indicate that mode water formation and subduction represent an efficient pathway for the transport of FDNPP-derived Cs into the ocean interior on 1-year timescales.

Figure 2

Time series of measured ^{137}Cs activities in surface seawater (*circles*) overlain on model-derived predictions (Tsubono et al. 2016) that includes ^{137}Cs levels from before the Fukushima Daiichi nuclear power plant releases. The color bar applies to both the observations and the model-derived predictions. The observations are from the Historical Artificial Radionuclides in the Pacific Ocean and Its Marginal Seas (HAM) database (Aoyama & Hirose 2004) and updates to that database (Buesseler et al. 2012; UNSCEAR 2014; IAEA 2015b, extracted and provided by P.J. Morris in March 2016; Yoshida et al. 2015; Aoyama et al. 2016), as well as unpublished data from J.N. Smith and Our Radioactive Ocean (**http://ourradioactiveocean.org/results**).


March 2011
October 2012
April 2011
April 2013
May 2011
April 2014
June 2011
April 2015
October 2011
April 2016
April 2012
137Cs activity (Bq m−3)
200
100
50
20
10
6
2
1
0.5
0.2
Latitude
30°N
15°N
0
150°E
180°
150°W
120°W
Longitude

Ocean circulation models all suggest that a broadening and diluting FDNPP radiocesium plume would have arrived in the eastern North Pacific in 2013–2014. Several of these simulations also predict maximum ^{137}Cs activities of 1–3 Bq m^{-3} to occur in North American coastal waters in 2015–2017 and then to gradually decline to levels of 1 Bq m^{-3} by 2020 (Behrens et al. 2012; Rossi et al. 2013, 2014). However, as noted above, FDNPP-derived ^{137}Cs activities of 10 Bq m^{-3} were measured at various locations in the eastern North Pacific in 2015, and no decreasing trend in most regions has been observed. One of the reasons for higher-than-predicted ^{137}Cs activities may be related to relatively weak mixing and strongly positive temperature anomalies in the eastern North Pacific starting in 2013–2014 caused by an unusual weather pattern that featured abnormally high sea-level pressure over this region (Bond et al. 2015). Conditions of less-intense mixing are consistent with observations of higher ^{137}Cs activities in offshore surface waters (as seen here) than would be predicted based on average mixing conditions. Despite these differences between empirical and model results, it is likely that FDNPP-derived ^{137}Cs activities will reach their maximum in 2015–2016, depending on the location, before declining by 2020 to levels of approximately 1–2 Bq m^{-3} associated with background fallout from nuclear weapons testing.

4. RADIONUCLIDES ASSOCIATED WITH SINKING PARTICLES

As noted above, only a small fraction of the FDNPP-derived radiocesium is associated with particulate organic matter and clay particles that may accumulate on the seafloor. In the case of the FDNPP releases, it was fortuitous that time-series sediment traps were already in place in the ocean off Japan in March 2011, collecting samples at two sites: K2 in the subarctic gyre (47°N, 160°E) and S1 in the subtropics (30°N, 145°E) (Honda et al. 2013) (**Figure 3*a***). Both locations had traps deployed at 500 and 4,810 m and were quite distant from the FDNPP site: 1,875 km northeast for K2 and 950 km southeast for S1, in water depths of 5,200 m and 5,800 m for K2 and S1, respectively.

Time-series sediment trap samples are collected in cups that open and close during programmed time intervals. At K2 and S1, trap samples collected between March 13 and 24, 2011, showed no detectable FDNPP signal, yet both sites showed FDNPP Cs (evidenced by ^{134}Cs) at 500 m after March 25, 2011, and one cup showed FDNPP Cs later, after April 6, 2011, in the deeper 4,810-m trap (Honda et al. 2013) (**Figure 3*b***). These findings lead to several conclusions. First, detection of a Cs signal so far from the FDNPPs so soon after the initial release suggests an atmospheric fallout Cs source, as ocean currents could not have carried Cs from the FDNPPs to these sites so quickly. Also, the difference in arrival times for Cs between 500 and 4,810 m allowed for an estimate of Cs sinking rates on particles of more than 180 m d^{-1}. Furthermore, the sediment trap data suggest that both the Cs flux and sinking rate were considerably lower after the first few months, with fluxes decreasing faster at 500 m to below the detection limit, and sinking rates decreasing to 50–70 m d^{-1} in 2012 (Honda & Kawakami 2014).

Two other studies measured FDNPP Cs (as evidenced by the presence of ^{134}Cs) in time-series sediment traps much closer to Japan, at site FS1, some 100 km due east of the FDNPPs (873-m trap in approximately 990-m water depth at 30°20′N, 142°10′E) (Otosaka et al. 2014), and site F1, some 100 km to the southeast of the FDNPPs (500- and 1,000-m traps in approximately 1,300-m water depth at 36°28′N, 141°28′E) (Buesseler et al. 2015) (**Figure 3*a***). Sample collections at F1 and FS1 were not initiated until 130 and 145 days after March 11, 2011, respectively, so they likely missed the first several months of higher FDNPP fluxes (**Figure 3*b***). The results at FS1 were similar to those at the more distant sites, with a maximum observed specific activity of ^{137}Cs of approximately 0.4 mBq kg^{-1} and sinking particles consisting mostly of biogenic mineral phases

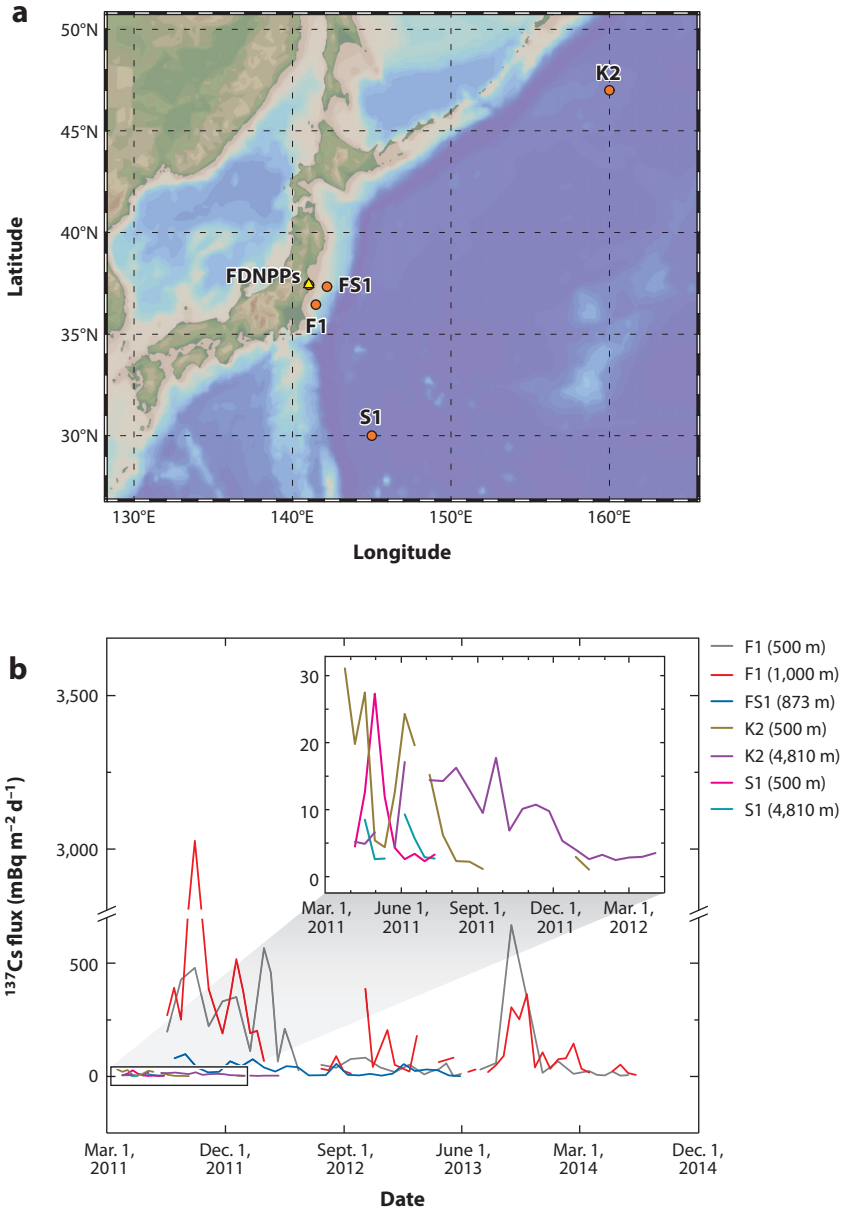


Figure 3

(*a*) Locations of the Fukushima Daiichi nuclear power plants (FDNPPs) and the F1, FS1, K2, and S1 time-series sediment traps. (*b*) Time-series flux of ^{137}Cs in sinking particles, as measured via sediment traps at four locations and at different depths. The inset shows an expanded *y*-axis scale that depicts the smaller fluxes observed in some of the traps.

and organic matter (Otosaka et al. 2014). However, with the much higher total mass flux in this coastal setting, total ^{137}Cs fluxes at FS1 were as high as 100 mBq m^{-2} d^{-1}, 3–4 times the earlier peak fluxes at K2 and S1. At FS1, the flux of Cs could be predicted from the water column activities and vertical scavenging associated with seasonal plankton blooms.

The even higher mass flux at F1 combined with much higher ^{137}Cs-specific activities on sinking particles (up to 1.8 mBq kg^{-1}) resulted in a ^{137}Cs flux that was more than 10 times that at FS1 and almost 100 times those at K2 and S1 (peak of 3,000 mBq m^{-2} d^{-1}) (**Figure 3*b***). Interestingly, Buesseler et al. (2015) noted that the lithogenic fraction in the sinking materials at F1 was approximately twice that found at FS1. Using ratios of ^{137}Cs to naturally occurring ^{210}Pb in the trap, they were able to show that, during periods of peak Cs input at F1, the sinking material resembled shelf sediments (higher ^{137}Cs/^{210}Pb and lithogenic fractions) and not local water column vertical scavenging. The 1,000-m trap had both higher Cs fluxes and a higher fraction of shelf-derived materials than the 500-m trap. The timing of peak Cs fluxes over a 3-year period suggested that typhoons were likely responsible for the resuspension of shelf sediments that were subsequently transported with the southward-flowing currents to the F1 trap site. When compared with the inventory of ^{137}Cs in coastal sediments, however, this laterally supported flux accounted for an annual loss term of 1% or less of the shelf sediment inventory.

In the first 6 months after the CNPP accident, Cs activities in traps in the North Sea (Kempe & Nies 1986), Black Sea (Buesseler et al. 1990), and Mediterranean Sea (Fowler et al. 1987) were on average much higher (1.3–5.2 mBq kg^{-1}) than those following the FDNPP event. The distance between the CNPP and these traps ranged from 600 to 2,200 km, so the higher activities resulted not from a closer proximity, but rather from a larger source term. It is also worth noting that the deep Black Sea trap (1,070 m) had higher fluxes than the shallow trap (250 m). This is similar to the measurements at the F1 site and suggests a lateral shelf source of sinking particles. Three other trap sites in the Bering Sea and North Pacific that were more than 8,000 km from the CNPP had radiocesium-specific activities and fluxes similar to those at the K2 and S1 traps following the FDNPP releases (Kusakabe et al. 1988). Looking back even further, to a time series of ^{137}Cs in a 4,000-m trap roughly 15 years after the peak in weapons-testing fallout in the early 1960s, Livingston & Anderson (1983) found ^{137}Cs activities of only 0.003–0.1 mBq kg^{-1} and fluxes of 0.02–1.6 mBq m^{-2} d^{-1} that increased with increasing water depth.

In summary, there are similarities and differences among all of the trap records. For both FDNPP and CNPP sources, rapid transport of radiocesium on sinking particles was observed in the upper few hundred meters of the ocean within 1–2 weeks after the accidents. Cs fluxes generally decreased quite rapidly after 3–6 months, with the exception of horizontally derived materials found at F1 and in the Black Sea deep traps. Comparisons of Cs fluxes on sinking particles with measurements of Cs water column inventories showed that the removal rates for FDNPP-derived Cs were less than 1–2% y^{-1} for FS1, S1, and K2 (Otosaka et al. 2014, Honda et al. 2013) and, similarly, 0.2–1% y^{-1} for the North, Black, and Mediterranean Seas after the CNPP accident (Kempe & Nies 1986, Buesseler et al. 1987, Fowler et al. 1987). These results support the above-mentioned finding that Cs is dispersed primarily via ocean currents on timescales of decades to centuries and is not very effectively scavenged from the water column.

5. RADIONUCLIDES IN SEAFLOOR SEDIMENTS

Seafloor sediments are important for the sequestration of particle-reactive radionuclides and serve as a contaminant reservoir for organisms that feed and live on the seafloor. They can also be a long-term source of contaminants through resuspension of fine-grained particle-bound radionuclides, bioturbation, and losses of soluble radionuclides from pore waters. Immediately following the

FDNPP releases, seafloor sampling and radionuclide analyses commenced as part of the Ministry of Education, Culture, Sports, Science, and Technology and TEPCO monitoring programs as well as several oceanographic field campaigns. Sediment sampling was conducted using surface grab samples and multicores that varied in their depth of penetration from less than 3 cm to more than 20 cm (Kusakabe et al. 2013, Otosaka & Kobayashi 2013, Ambe et al. 2014, Black & Buesseler 2014, Otosaka & Kato 2014). A towed gamma ray spectrophotometer that measured the average radioactivity within approximately the top 3 cm of sediment was also deployed to study small-scale variability in Cs sediment distributions (Thornton et al. 2013).

Radioactive contamination in bottom sediments from sites off the east coast of Japan were dominated by ^{134}Cs and ^{137}Cs (Kusakabe et al. 2013, Otosaka & Kobayashi 2013, Thornton et al. 2013, Ambe et al. 2014, Black & Buesseler 2014, Otosaka & Kato 2014, Sohtome et al. 2014, Nagaoka et al. 2015). Although Pu and Am are more particle reactive in their geochemistry, measurements of their activities and isotopic ratios in sediments reflect atmospheric weapons testing rather than a smaller FDNPP source (Zheng et al. 2012, Bu et al. 2013, Wu et al. 2014, Oikawa et al. 2015). ^{90}Sr was released in much higher concentrations than Pu, but inventories of ^{90}Sr in bottom sediments are likely three orders of magnitude lower than the ^{90}Sr inventories measured in the water column owing to the low affinity of ^{90}Sr to particles (Periáñez et al. 2013). Given the relatively small inputs of FDNPP-derived Pu, Am, and ^{90}Sr and the decay of ^{134}Cs (less than 20% of the initially released ^{134}Cs remains after 5 years), the discussion below focuses on seafloor ^{137}Cs distributions.

Sedimentary ^{137}Cs varies substantially both temporally and spatially, with inventories ranging from those expected from nuclear weapons testing (less than 50 Bq m^{-2}) (Ito et al. 2007) to more than 100,000 Bq m^{-2} in sediments closest to the FDNPPs (**Figure 4**). In general, ^{137}Cs inventories decrease with increasing distance from the FDNPPs and increasing water depth because of lower water column particle abundances that result in decreased removal on sinking particles offshore. As a result of the southward-flowing currents and finer-grained sediments, radiocesium inventories are somewhat higher in shelf sediments to the south of the FDNPPs relative to the north (Kim et al. 2006, Otosaka & Kobayashi 2013, Ambe et al. 2014, Black & Buesseler 2014, Ono et al. 2015). These trends, however, are confounded by high spatial variability in ^{137}Cs activities, which can span a factor of 3–5 even within one set of multicore samples collected simultaneously and immediately adjacent to one another (e.g., Black & Buesseler 2014).

Whether associated with clay minerals or organic material, once deposited on the seafloor, Cs may be remobilized in its particle-associated state and transported horizontally by physical processes, and/or redistributed and mixed vertically, largely by bioturbation. Finer-grained sediments are more easily resuspended and transported via currents, as observed in particle flux data that showed a greater degree of shelf sediment input following typhoon events (Buesseler et al. 2015; see also Section 4 on sediment traps). Thornton et al. (2013) further argued that bottom topography may shield fine-grained sediments from advective currents in certain areas, thereby confining contaminants to the initial area of deposition. These physical redistribution processes help to explain the transport of Cs to the southern coastal region as well as the large spatial variability observed in sediments.

Bottom-feeding and bottom-dwelling organisms are more abundant near the shore, where they can further affect Cs biogeochemistry in surface sediments. Black & Buesseler (2014) derived bioturbation rates using ^{210}Pb and found substantially higher mixing rates in the most Cs-contaminated sediments of the southern coastal region, with decreasing mixing to the north and offshore. They estimated that 50% of Cs-contaminated sediments in the southern coastal region would be mixed deeper than 3 cm within a year of deposition, whereas to the north and offshore, lower bioturbation rates resulted in a much slower decline in surface Cs activities (a

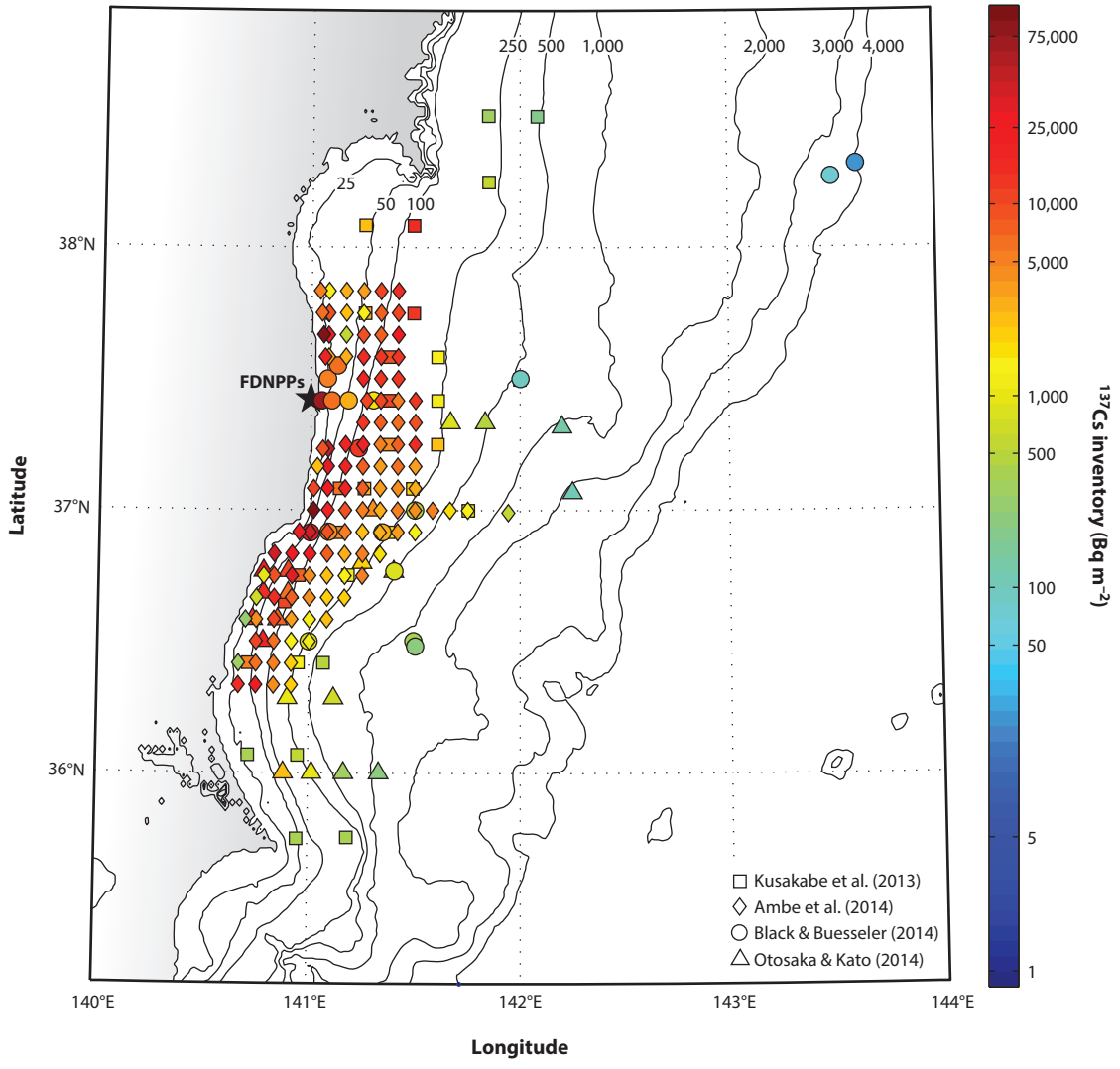


Figure 4

Compilation of ^{137}Cs inventories from the seafloor off Japan from cores collected in 2012 and 2013. If multiple cores were collected at the same position, data were averaged. The site of the Fukushima Daiichi nuclear power plants (FDNPPs) is shown by the black star, and depth contours are plotted in meters. For details of sampling and calculation of inventories, see Kusakabe et al. (2013), Ambe et al. (2014), Black & Buesseler (2014), and Otosaka & Kato (2014).

50% decrease would take 10–25 years). Thus, bioturbation may prove to be an effective mechanism for reducing overall Cs concentrations at the sediment surface over shorter timescales and constraining radiological impacts on surface-dwelling infauna. However, bioturbation also represents a mechanism for the return of deeper, albeit Cs-depleted, sediments to the sediment surface. Thus, bioturbation may provide a continuing source of FDNPP Cs contamination at the sediment-water interface over much longer timescales than would be predicted based solely on local sedimentation rates.

Whereas bioturbation can cause a decline in surface sediment activities, bioirrigation can increase pore water exchange with bottom waters. Uptake of Cs in clay lattices, especially illites, is essentially irreversible in freshwater systems, but it can undergo some degree of desorption in higher-ionic-strength media such as seawater (Staunton & Roubaud 1997). In fact, Cs is enriched in pore waters in coastal sediments (Sholkovitz & Mann 1984), in which case diffusion and bioirrigation could govern the transport of dissolved Cs to the overlying waters. This has been observed in the Irish Sea, where, following large reductions in ^{137}Cs releases from Sellafield, desorption of Cs from sediments became a major source to the water column. Poole et al. (1997) reported that approximately 4% of sediment ^{137}Cs was returned in aqueous phases to the Irish Sea annually. These observations illustrate the complexity of Cs associations with particle surfaces.

In the broadest sense, ^{137}Cs sediment activities off Japan reflect a combination of source, mineralogy, local currents, and water column and benthic biological activity. In total, seafloor sediments contain less than 1% (130 $\pm$ 60 TBq) of the ^{137}Cs activity initially released from the FDNPPs (Kusakabe et al. 2013, Black & Buesseler 2014). However, given the gradual decrease in Cs concentrations in the water column since the initial FDNPP release, the sediment repository is now more than 5–10 times larger than the current total inventory of Cs in the overlying waters (36–38°N, at water depths of up to 200 m) (Buesseler 2014). Rapid downward mixing of Cs-contaminated sediments by bioturbation helps to reduce surface Cs sediment concentrations and reduce biological uptake at the sediment-water interface, but bioturbation can also return contaminated sediments to the surface on timescales of years to decades. Physical resuspension of sediments will reduce Cs activities by dispersion offshore, and soluble losses will occur. However, continued inputs of sediment-bound Cs from rivers and groundwater essentially balance those losses, resulting in small expected changes to sediment inventories. These results therefore suggest that the nearshore sediments off Japan will remain a significant long-term source of radiocesium for years to decades, depending on the location and sediment type, although more study is needed to constrain these source and loss terms. This is consistent with previous studies examining radiocesium contamination from Sellafield in the Irish Sea, where, after inputs were dramatically reduced, the inventory of total sediment ^{137}Cs declined by half on timescales of approximately 5–20 years (e.g., Mitchell et al. 1999).

6. MARINE BIOTA UPTAKE OF AND EXPOSURE TO RADIONUCLIDES

Once released to the environment, radionuclides can be rapidly incorporated into marine organisms either by uptake from seawater or by food ingestion (Fowler & Fisher 2004). By the end of March 2011, the Japanese authorities had begun conducting gamma analyses of marine organisms for radioprotection purposes. Several thousand results have now been reported on the websites of the Ministry of Agriculture, Forestry, and Fisheries and TEPCO (MAFF 2015, TEPCO 2016). Although most of the biota sampling has been made by the Japanese authorities, several independent radioecological studies have also been conducted since the accident (Fisher et al. 2013, Tateda et al. 2013, Johansen et al. 2014, Vives i Batlle et al. 2014).

Cs is most often measured in the edible part of fish, because Cs, like K, is enriched in fish flesh. Because the flesh represents the largest component of fish body weight, these analyses provide a good estimate of total Cs and are the most relevant values for human consumers. In the weeks following the accident, relatively high Cs activities of up to several hundred thousand becquerels per kilogram wet weight (ww) were found in some species of fish caught in the coastal waters of the Fukushima Prefecture, although the vast majority had activities of less than 1,000 Bq kg^{-1} ww (**Figure 5**). Prior to the FDNPP releases, the regulatory limit for radiocesium in seafood in Japan was 500 Bq kg^{-1} ww; on April 1, 2012, the Japanese authorities lowered this limit to 100 Bq kg^{-1} ww (see Section 7 and **Table 2**).

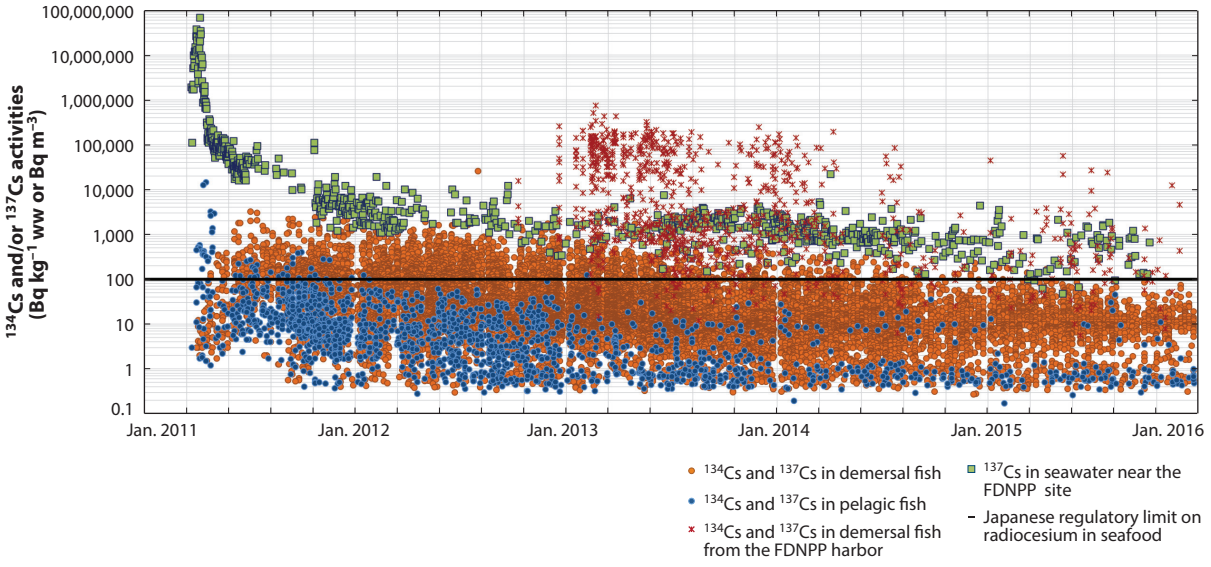


Figure 5

Total ^{134}Cs and ^{137}Cs activities in various pelagic and demersal fish from the coastal waters of several Japanese prefectures (Aomori, Chiba, Fukushima, Hokkaido, Ibaraki, Iwate, and Miyagi) and from within the Fukushima Daiichi nuclear power plant (FDNPP) harbor as a function of time. Also plotted are ^{137}Cs activities in seawater collected close to the FDNPPs (at site F1). The black line shows the Japanese regulatory limit for total radiocesium in seafood [100 Bq kg^{-1} wet weight (ww)]. The pelagic fish are amberjack, anchovy, dory, halfbeak, herring, icefish, mackerel, sandlance, sardine, saury, and smelt; the demersal fish are cod, conger, flounder, greenling, hakeling, halibut, jacopever, monkfish, plaice, pollock, rockfish, skate, and sole.

In 2011, approximately half the fish sampled in coastal waters off Fukushima Prefecture had radiocesium levels above 100 Bq kg^{-1}, and approximately 10% were below the detection limit of approximately 7 Bq kg^{-1}. By 2015, the situation was reversed: Fewer than 1% of measurements in fish had radiocesium levels above 100 Bq kg^{-1}, and 80% of measurements were below the detection limit (MAFF 2015, TEPCO 2016). Such data are used to set in-place fishing bans recommended by the MAFF and Japanese government that are now being lifted for certain areas and species as activities drop below regulatory limits.

In general, demersal fish, which live and feed in close proximity to bottom sediments, have higher Cs activities than pelagic fish, and specimens of both types caught off of Fukushima Prefecture have levels higher than those in prefectures located north or south of the FDNPPs

Table 2 Regulatory limits for radiocesium in seafood in Japan, the United States, and the European Union

Government	Limit[a]
Japan (after April 1, 2012)	100
Japan (before April 1, 2012)	500
United States	1,200
European Union	1,250

[a]Total ^{134}Cs + ^{137}Cs becquerels per kilogram wet weight.

(Buesseler 2012) (**Figure 5**). Some of the highest Cs activities found in fish in coastal waters (25,800 Bq kg^{-1} ww) were measured in two greenlings caught close to the Ota River in August 2012 that were thought to have migrated from the FDNNP harbor (Shigenobu et al. 2014, Fujimoto et al. 2015). Indeed, by October 2012, TEPCO had reported extremely high Cs activities—up to thousands of becquerels per kilogram wet weight in various demersal species sampled in the FDNPP harbor (**Figure 5**). Some fish caught within the harbor remain highly contaminated even 5 years after the accident and are now prevented from leaving the contaminated area by a net. These higher sustained Cs activities are likely due to the close proximity of the fish to both the leaking FDNPP reactors and highly contaminated sediment in the harbor area. By comparison, after the CNPP accident, ^{137}Cs concentrations in the range 30,000–180,000 Bq kg^{-1} ww were reported for freshwater fish near the CNPP (e.g., Kryshev 1995).

The ability of an organism to accumulate an element is often expressed through the use of a concentration factor—in this case, the ratio of the organism activity (becquerels per kilogram wet weight) to seawater activity (becquerels per kilogram or becquerels per liter). The underlying assumption is that organisms are in equilibrium with their ambient seawater with respect to the radionuclide concentration. The concentration factor for Cs in fish (irrespective of the species) is approximately 100 (IAEA 2004). This is a moderately low value compared with those of some other elements (e.g., iron and tin, which can have concentration factors as high as 3×10^4 and 5×10^5, respectively) and other contaminants [e.g., mercury and polychlorinated biphenyls (PCBs)] (Harmelin-Vivien et al. 2012). Cs also has a limited biomagnification in marine food chains (only a factor of approximately 2) (Kasamatsu 1997, Zhao et al. 2001, Heldal et al. 2003, Mathews & Fisher 2008, Harmelin-Vivien et al. 2012).

All of the fish data collected after the initial FDNPP release show high variability in Cs activity for a given date and location, which can be linked to several factors, including variability in the ocean (both water and sediment), fish habitat, fish diet, fish size (Cs activities are known to increase with increasing size), fish mobility, and consequent exposure history. Despite this variability, the large amount of data gathered over several years reveals a gradual, systematic decrease in radiocesium activities over time in marine biota (**Figure 5**). For organisms in natural settings, this decrease is quantified by the ecological half-life, i.e., the time required for a 50% decline in organism radionuclide activity. Indeed, Cs levels decrease by a factor of 2 in just a few months in various planktivorous fish and their predators, and closer to a year in various coastal demersal fish at higher trophic levels (Iwata et al. 2013, Tateda et al. 2015, Tagami & Uchida 2016). This decrease in Cs activities in some demersal fish species is taking longer than predicted, which has been attributed to continuing contamination of their food source (benthic infauna) from sediments (see discussion above) (Buesseler 2012, Tateda et al. 2013, Wada et al. 2013, Sohtome et al. 2014, Tateda et al. 2015). Ecological half-lives on the order of 100 days for bivalves and gastropods and on the order of several hundred days for polychaetes have been reported (Iwata et al. 2013, Wada et al. 2013, Sohtome et al. 2014).

Several other FDNPP-derived radionuclides have been detected in marine biota, but they have either disappeared quickly because of decay or are present at much lower activities because of their relatively lower release ratios and/or lower concentration factors in marine biota. For example, very high ^{131}I activities (several hundred to several thousand becquerels per kilogram wet weight) were measured in marine biota in April 2011 (MAFF 2015). ^{131}I is important from a radiological perspective because it is a major contributor to the dose received by organisms; however, its short half-life results in activities that have been below the detection limit in marine biota since mid-July 2011.

Although ^{110m}Ag has not been reported in the FDNPP releases, it was detected systematically in zooplankton sampled off Japan in June 2011 (Buesseler et al. 2012). It was also detected in

some crabs and molluscs sampled in coastal areas, with a clear decline in activities with increasing distance from the FDNPPs (Horiguchi et al. 2016, TEPCO 2016), but was not detectable in fish samples. Silver is known to be actively incorporated by marine biota (concentration factors in the range 10^4 to 6×10^5; IAEA 2004), but it has a low assimilation efficiency in marine fish (Pouil et al. 2015). ^{110m}Ag was also reported in biota from the Mediterranean and Baltic Seas after the CNPP accident (e.g., Calmet et al. 1991, Carlson & Holm 1992).

^{90}Sr was also released during the FDNPP accident (see Section 2) and would be expected to accumulate in fish bones, given its geochemical similarity to calcium. However, because the initial ocean activities of Sr were much lower than those of ^{137}Cs, and because Sr is much more difficult to measure, this element has been less well studied. Concentration factors for Sr in marine biota are extremely low (in the range of 1–10; IAEA 2004), leading to low activities of a few becquerels per kilogram wet weight or less in various fish species (MAFF 2015, TEPCO 2016). This is only slightly above pre-FDNPP release levels, which were around 0.02–0.07 Bq kg^{-1} ww (Johansen et al. 2014, Fujimoto et al. 2015). However, higher activities were reported for rockfish caught within the FDNNP harbor. There, ^{90}Sr concentrations were proportional to Cs activities, with a mean ^{137}Cs/^{90}Sr ratio close to 300 (Fujimoto et al. 2015).

Pu was released in only small amounts from the FDNPPs (see Section 2) (Evrard et al. 2015). As such, only a few data are available for Pu in fish. These results do not show any measurable FDNPP-derived Pu in marine biota relative to earlier data (Yamada et al. 1999, FAJ 2015).

What can be said about possible dose effects on marine biota? Organisms inhabiting areas contaminated by the FDNPPs receive external irradiation from radionuclides in water and sediment and receive internal radiation from radionuclides ingested via food and water and, in some cases, absorbed through the skin and respiratory systems. In coastal areas, absorbed dose rates of up to 4,600 mGy d^{-1} for macroalgae and 2,600 mGy d^{-1} for benthic biota (fish, molluscs, and crustaceans) were estimated from exposure to ^{131}I, ^{134}Cs, and ^{137}Cs (both internal and external) during the first month after the initial FDNPP release, assuming equilibrium with ambient radionuclide activities (Garnier-Laplace et al. 2011). However, subsequent studies have shown that these estimates were likely an overestimate, as Cs and ^{131}I activities declined rapidly (Buesseler et al. 2011, Kryshev & Sazykina 2011, Kryshev et al. 2012).

An international assessment was conducted for marine biota under the United Nations Scientific Committee on the Effects of Atomic Radiation (UNSCEAR 2014, Vives i Batlle et al. 2014) based on the monitoring data collected between May 2011 and August 2012 and taking into account two time stages: an acute exposure phase lasting for a few weeks immediately after the FDNPP releases and a chronic exposure phase at a lower dose rate lasting for 90 days to 1 year. During the acute phase, the various marine biota dose estimates are far below (or on the same order of magnitude for macroalgae) the ERICA (Environmental Risk from Ionising Contaminants: Assessment and Management) acute benchmark value of approximately 5 Gy, which is considered to be of concern for marine biota. During the second phase, the weighted absorbed dose rates (^{134}Cs, ^{137}Cs, and ^{131}I, both internal and external) were highly variable depending on location but were also well below the 0.24 mGy d^{-1} ERICA benchmark for chronic exposure (below which no effects are expected at the population level) (Garnier-Laplace & Gilbin 2006). However, in the FDNPP harbor, this benchmark was reached and continued to be exceeded even 3 years after the initial FDNPP release for various species (i.e., median dose rate of 1.1 mGy d^{-1} and maximum of 4.3 mGy d^{-1}; Johansen et al. 2014).

In the open ocean, very low Cs dose rates were received by planktonic populations both within 30 km of the FDNPPs (Belharet et al. 2016) and beyond (i.e., 30–600 km) (Fisher et al. 2013). Pacific bluefin tuna caught off the California coast in August 2011 (Madigan et al. 2012) were

calculated to have received an internal dose close to 0.24 μGy d^{-1} when they were in Japanese waters for 3 months prior to migration (Fisher et al. 2013).

Dose assessments have several limitations, including a lack of information about the activities of short-lived radionuclides in the first days after the initial FDNPP release. That said, it is likely that the dose rates stayed below levels at which radiation effects could be observed, with the exception of the FDNPP harbor. A recent study documenting a decline in the number of species and population densities of intertidal biota between 2011 and 2013 in the region closest to the FDNPPs identified several potential causes, including direct impacts from the tsunami and toxicity from both chemical and radiological sources (Horiguchi et al. 2016).

In summary, there has been a significant decrease in the number of fish above the radiocesium limit of 100 Bq kg^{-1} ww over the past 5 years, from more than 50% down to less than 1%. However, ^{137}Cs activities in marine biota are still above pre-FDNPP background levels. As expected, marine biota were more contaminated in the coastal waters near the FDNPPs, and pelagic fish proved to be less contaminated than demersal fish. Fish diet and foraging behavior in sediment are additional factors that should be examined more closely (Johansen et al. 2014). Even though the environmental risks associated with fish that exceed 100 Bq kg^{-1} ww were extremely low by 2016 (Little et al. 2016, Okamura et al. 2016), a better understanding of the processes that led to long ecological half-lives in certain species of demersal fish is essential. With the exception of marine biota in close proximity to the FDNNPs, calculated doses have generally indicated no potential for effects on marine biota populations.

7. RADIOLOGICAL DOSES TO HUMANS AND SOCIETAL IMPACTS

To address public radiological concerns related to FDNPP sources and the oceans in particular, one needs to consider that individuals are exposed to radionuclides through multiple pathways, including inhalation of particles and ingestion and direct exposure arising from the surrounding environment. Contributors to the total dose include radiation from natural sources, medical procedures, and industrial and governmental activities (**Figure 6**, **Table 3**). The total radiation dose received by an individual is the sum of these pathways of exposure and is expressed as the effective dose.

The added dose from the FDNPPs should be discussed relative to the global average dose from natural background radiation, which is approximately 2.4 mSv y^{-1} (Thorne 2003). This can be apportioned into 1.2 mSv y^{-1} from inhaled radionuclides (primarily radon gas), 0.29 mSv y^{-1} from ingested radioactivity, 0.39 mSv y^{-1} from cosmic radiation, and 0.48 mSv y^{-1} from radiation arising from the surrounding geology (UNSCEAR 2008). Globally, natural background varies, primarily because of elevation, latitude, and the underlying geology. Exposures worldwide from natural sources are estimated to fall within the range of 1–13 mSv y^{-1}, although there are exceptions (UNSCEAR 2008). High natural background radiation can exceed 50 mSv y^{-1} in locations such as Ramsar, Iran; Guarapari, Brazil; Kerala, India; and Yangjiang, China (Aliyu & Ramli 2015).

Diagnostic imaging and interventional medical procedures that use ionizing radiation can deliver doses that range from 0.01 to 70 mSv per procedure (Mettler et al. 2008). In the United States, for instance, the increased use of radiation in medicine has resulted in a near doubling of the average annual dose, from 3.6 mSv in 1980 to 6.2 mSv in 2006, making medical use the single largest contributor to dose (Schauer 2009). The use of radiation in cancer treatment (radiotherapy) uses much higher doses (up to 12,000 Gy) during attempts to kill cancer cells (Cancer Netw. 1999).

Radiation exposure also comes from industrial and governmental practices. Radionuclides released from past nuclear weapons tests have a global footprint. The levels are substantially lower

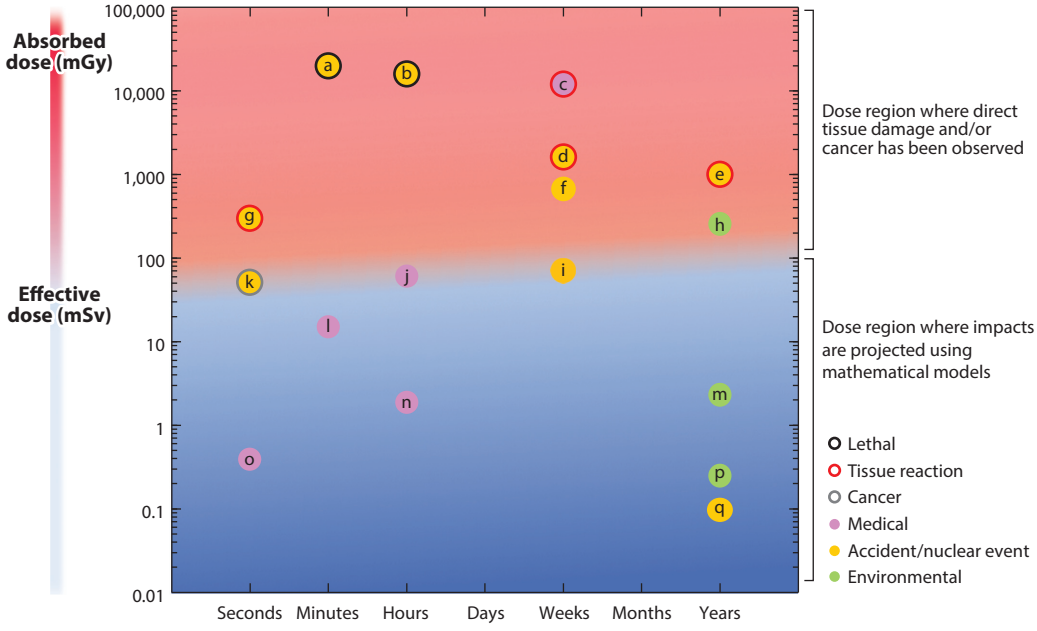


Figure 6

Plot of dose and duration of exposure for a variety of different medical, accidental, and environmental sources. **Table 3** lists the sources and references that correspond to the lettered data points. The background shading shows dose regions where impacts are projected by mathematical models (*blue*) and where direct tissue damage and/or cancer has been observed (*red*). The boundary between these regions is not a sharp line, and it also roughly separates the common use of effective dose [as quantified in units of millisieverts (10^{-3} Sv)] and specific absorbed energy [used when effects include tissue damage, as quantified in units of milligrays (10^{-3} Gy)].

than they were during the 1960s, and the current global average contribution to dose is estimated to be less than 0.005 mSv (UNSCEAR 2008). By comparison, the routine operations of nuclear power plants contribute a dose of less than 0.0002 mSv y^{-1} to the general population (UNSCEAR 2008, Mettler et al. 2009).

Radionuclides in foodstuffs represent only approximately 5–10% of an individual's dose. Public exposure to naturally occurring radionuclides in food comes largely from ^{40}K and radionuclides in the U and Th series, contributing approximately 0.3 mSv y^{-1}. The total dose varies globally and ranges from 0.2 to 1 mSv y^{-1} (UNSCEAR 2008).

The dose received from radioactivity in food depends on both the age of the individual and the specific characteristics of the radionuclide. Dose coefficients, expressed in millisieverts per becquerel, are used to calculate effective dose (Eckerman et al. 2013). For example, a 3-month-old infant will receive a dose of 2×10^{-5} mSv Bq^{-1} from the ingestion of 1 Bq of ^{137}Cs, whereas an adult will receive 1.3×10^{-5} mSv from the same amount of ^{137}Cs. The total dose received annually from food consumption is the radionuclide concentration in food (in becquerels per kilogram) multiplied by the dose coefficient (in millisieverts per becquerel) and the total amount of food consumed (in kilograms). Agencies such as the Food and Agriculture Organization of the United Nations make estimates of annual dietary intake by food class (dairy, meat fish, produce, etc.) and age to estimate annual food intake (in kilograms per year). These data, along with the fraction of food assumed to be contaminated and a target dose, allow organizations to estimate specific limits of radionuclide activities in foodstuffs, known as derived intervention levels (expressed in becquerels per kilogram) (FAO & WHO 1994, ICRP 2007).

Table 3 Data points shown in Figure 6

Data point	Category	Absorbed or effective dose (exposure duration)	Description	Documented health impact
a	Accident/nuclear event	20,000 mGy (minutes to hours)	Dose during Tokaimura criticality (Hayata et al. 2001)	Lethal
b	Accident/nuclear event	16,000 mGy (hours)	Dose to Chernobyl workers (UNSCEAR 2000)	Lethal
c	Medical	12,000 mGy (weeks)	Total body irradiation (Lawton 1998)	Immune suppression
d	Accident/nuclear event	1,600 mSv (weeks)	Maximum dose to infant Chernobyl evacuees (Pröhl et al. 2002, Balonov et al. 2007)	Functional thyroid changes and thyroid cancer
e	Accident/nuclear event	1,000 mGy (years)	Chronic exposure at the Mayak and Techa Rivers (Standring et al. 2009)	Hematopoietic impairment
f	Accident/nuclear event	670 mSv (weeks)	Maximum dose to Fukushima workers (WHO 2013)	None observed—estimated
g	Accident/nuclear event	300 mGy (seconds)	Dose to fetuses at Hiroshima (Otake 1996)	Mental deficit
h	Environmental	260 mSv (years)	Natural background radiation in Ramsar, Iran (Aliyu & Ramli 2015)	Unclear
i	Accident/nuclear event	70 mSv (weeks)	Dose to Fukushima evacuees (WHO 2013)	None observed—estimated
j	Medical	60 mSv (hours)	Dose during a pelvic vein embolization (Mettler et al. 2008)	None observed—estimated
k	Accident/nuclear event	50 mSv (seconds)	Lowest dose where clear evidence of cancer has been documented from acute exposure in Japanese atomic bomb survivors (Brenner et al. 2003)	Cancer
l	Medical	15 mSv (minutes or hours)	Dose during a CT scan for pulmonary embolism (Mettler et al. 2008)	None observed—estimated
m	Environmental	2.4 mSv (years)	Global average natural background (UNSCEAR 2000)	None observed—estimated
n	Medical	1.9 mSv (hours)	Dose during a thyroid scan using ^{99m}Tc (Mettler et al. 2008)	None observed—estimated
o	Medical	0.4 mSv (seconds)	Dose during a mammogram (Mettler et al. 2008)	None observed—estimated
p	Environmental	0.25 mSv (years)	^{210}Po dose from consumption of shellfish (Pentreath & Allington 1988, Alam & Mohamed 2011)	None observed—estimated
q	Accident/nuclear event	<0.1 mSv (years)	Intervention level established to control dose from consumption of food from Fukushima (Harada et al. 2013)	None observed—estimated

Prior to the initial FDNPP release in 2011, fission radionuclides such as ^{137}Cs and ^{90}Sr were detectable worldwide in foodstuffs, primarily because of fallout from past nuclear weapons tests. Following the CNPP accident in 1986, the concentrations of fission products such as ^{131}I, ^{137}Cs, and ^{90}Sr in foodstuffs in Ukraine were more than 1,000 times the baseline fallout concentrations (Nesterenko et al. 2010). As with observations of fallout, once these and other anthropogenic radionuclides were released into the environment, their activities steadily decreased owing to a combination of radioactive decay and biological and geochemical redistributions (e.g., Landis et al. 2012).

Following the FDNPP releases, measurements of radionuclides in foodstuffs were made by researchers, the public, and government agencies of many countries as they sought to provide information to a concerned public. The Japanese government instituted regulations to measure radionuclides in, and restrict consumption of, potentially contaminated foodstuffs (Hamada et al. 2012). As mentioned above, the Japanese authorities also reduced the regulatory limit for radiocesium in seafood from 500 to 100 Bq kg^{-1} ww on April 1, 2012, in an attempt to reassure Japanese consumers that their food had the world's highest standards for radiological safety. For comparison, limits in the United States and the European Union are set at 1,200 and 1,250 Bq kg^{-1} ww, respectively (**Table 2**).

As reviewed above, the highest radiocesium activities were found in demersal fish in the FDNPP harbor (**Figure 5**). Many other species exhibited activities above 100 Bq kg^{-1} in the first year after the FDNPP releases (e.g., Buesseler 2012) (**Figure 5**). Povinec & Hirose (2015) estimated the effective dose for someone ingesting seafood from off the coast of the FDNPPs between 2011 and 2013 to be 0.6 $\pm$ 0.4 mSv y^{-1}, as compared with a dose of 0.7 mSv y^{-1} from naturally occurring ^{210}Po in fish and shellfish. This is in agreement with Johansen et al. (2014), who calculated a dose of 0.13 mSv y^{-1} from radioactive Cs for a hypothetical consumer of 50 kg of fish collected in 2013 within 3 km of the FDNPPs. The dose from ^{90}Sr is calculated to be three orders of magnitude less than the corresponding dose rates from Cs in seafood (Maderich et al. 2014). All of these studies confirm prior work showing that, in general, ^{210}Po remains the major contributor to the dose received from seafood consumption (Aarkrog et al. 1997).

Anthropogenic radionuclides have also been detected in very small quantities in foodstuffs along the west coast of North America. For example, ^{131}I was detected in *Fucus* seaweed in Vancouver, Canada, at a maximum activity of 4,930 Bq kg^{-1} following the CNPP accident; shortly after the FDNPP releases, seaweed from the same general area had activities of 130 Bq kg^{-1} (Chester et al. 2013). Pacific bluefin tuna (*Thunnus orientalis*) caught off San Diego in August 2011 had detectable ^{134}Cs and ^{137}Cs activities of 4 and 6 Bq kg^{-1} ww, respectively (Madigan et al. 2012), whereas albacore (*Thunnus alalunga*) caught off the US Pacific Northwest coast in 2012 had even lower ^{134}Cs and ^{137}Cs activities (0.02–0.4 and 0.2–0.8 Bq kg^{-1} ww, respectively) (Neville et al. 2014). None of these activities in fish result in significant doses (10–20 $\times$ 10^{-9} Sv per kilogram consumed).

It is well documented that radiation exposure can cause cancer or other health effects (ICRP 2007). At high doses and dose rates, certain tissue reactions (such as skin burns and organ failure) and even death can occur. In recognition of these effects, radiation limits for workers and the public have been established to prevent such reactions and minimize the potential for cancer induction. Although substantive epidemiological data indicate an increased cancer risk from acute doses exceeding 50 mSv, distributing the dose over time appears to lower the risk (Brenner et al. 2003). The epidemiological data support an increase in cancer risk from protracted exposures exceeding 100 mSv (Brenner et al. 2003). There are considerable uncertainties in the risk projections, but radiation safety advisory bodies such as the International Commission on Radiological Protection currently estimate the risk of fatal cancer from radiation exposure to the general population to be 5% Sv^{-1} (ICRP 2007), equivalent to 1 fatal cancer arising per 20,000 people exposed to 1 mSv.

It is important to note that the variation in cancer incidence across human populations—resulting from their environment, lifestyle choices, sensitive subpopulations, and genetics—makes unequivocal determination of risks at doses of less than 50–100 mSv problematic and inconclusive. **Figure 6** illustrates the range of exposures that occur from medical practices, naturally occurring radiation, and accidents or nuclear events, including those at Chernobyl, Tokaimura, Hiroshima and Nagasaki, and Fukushima. The baseline incidence of fatal cancer in the United States is approximately 20%, which means a total lifetime cancer mortality rate of 1 in 5 (Natl. Cancer Inst. 2016). The lifetime risk of cancer mortality in Japan is slightly higher, approximately 24% (Ogino & Hattori 2014). The Fukushima region evacuees with the greatest exposure received a total dose of 70 mSv, which (if they are representative of the general population) would increase their fatal cancer risk from 24% to 24.4%.

Although there have been no direct casualties attributed to radiation exposure, more than 15,000 died or went missing as a result of the tsunami and earthquake. However, the societal impacts of a nuclear event go far beyond the direct radiological impacts. Evacuation and long-term relocation have been linked to psychological effects and stress-related casualties (on the order of 2,000–3,000 deaths) (Tanigawa et al. 2012, Ohtsuru et al. 2015). Of the more than 160,000 people evacuated from the area, approximately 100,000 are still classed as evacuees (Fukushima Prefect. 2016a,b), a number that includes many from coastal areas that suffered from both the tsunami and the nuclear accident. In addition to the designated evacuation areas, many regions experienced voluntary relocation, with younger generations more likely to move and the elderly more likely to remain (IAEA 2015a). This led to demographic changes and concerns about whether younger generations would take over family businesses. Fishing communities were particularly affected by experiencing loss of livelihood and lack of consumer trust in their products. Although the strict controls on foodstuffs meant that internal doses to populations were extremely low, all food industries suffered from loss of consumer trust in all Fukushima Prefecture products, with market prices dropping to 50% of those in other areas (Fukushima Prefect. 2016b), as well as export losses. Fishery production numbers from 2011 to 2013 were down to a third of those from previous years (Fukushima Prefect. 2016b). Tourist and cultural activities were similarly affected, with the region experiencing a 20% drop in visitors for the 2 years following the accident (IAEA 2015a, Fukushima Prefect. 2016b).

In recent years, both market prices and tourist numbers have recovered, and by 2015, a number of towns had been cleared for the return of populations, including the coastal towns of Hirono and Naraha to the south of the FDNPPs and areas in Minamisoma to the north. As in other areas in Fukushima, the return rate has been low and dominated mostly by the elderly. However, many families have reported that, in deciding whether to return, the lack of infrastructure (such as hospitals and schools) and employment opportunities is at least as important as (and sometimes more important than) concerns about radiation (IAEA 2015a). Recognizing this distinction has been an important part of the recovery plans for Fukushima, which deal not only with radiation protection measures, but also with industry and community revitalization. Although one cannot expect a total return of the communities to their status before March 11, 2011, it is hoped that, with time, a new normality will return to the affected areas and that an improved understanding of the fate and impacts of radionuclides discharged to the oceans will help to contribute to that recovery.

DISCLOSURE STATEMENT

K.B. has served in a consulting capacity related to radionuclides in Japanese fisheries products.

ACKNOWLEDGMENTS

We thank the Scientific Committee on Oceanic Research and the offices of Ed Urban for support for travel and meetings of Working Group #146 (Radioactivity in the Ocean, 5 Decades Later; **http://www.whoi.edu/CMER/rio5-working-group**), which, along with the North Pacific Marine Science Organization through Working Group #30 (Assessment of Marine Environmental Quality of Radiation Around the North Pacific), supported open-access publication for this article. K.B. was supported in part by the Gordon and Betty Moore Foundation and the Deerbrook Charitable Trust. P.M. was supported in part by the Generalitat de Catalunya through MERS (grant 2014 SGR 1356), the European Commission 7th Framework COMET-FRAME project (grant agreement 604974), and the Ministerio de Economía y Competitividad of Spain (project CTM2011-15152-E). S.C. was supported in part by the French program Investissement d'Avenir run by the National Research Agency (AMORAD project, grant ANR-11-RSNR-0002). D.O. was supported in part by the Center for Environmental Radioactivity (NFR Centers of Excellence grant 223268/F50). J.N.S. was supported in part by the Marine Environmental Observation, Prediction, and Response Network. The International Atomic Energy Agency is grateful to the Government of the Principality of Monaco for the support provided to its Environment Laboratories. The MARiS database provided data for Section 3 (IAEA 2015b). The contents of this paper are solely the opinions of the authors and do not constitute a statement of policy, decision, or position on behalf of the International Atomic Energy Agency.

Affiliations for the coauthors of this article are as follows:

[2]State Key Laboratory of Marine Environmental Science, Xiamen University, Xiamen 361102, China; email: mdai@xmu.edu.cn

[3]Institute of Environmental Radioactivity, Fukushima University, Fukushima 960-1296, Japan; email: r706@ipc.fukushima-u.ac.jp

[4]University of South Carolina, Columbia, South Carolina 29208; email: cbnelson@geol.sc.edu

[5]Institut de Radioprotection et de Sûreté Nucléaire, PRP-ENV, La Seyne/Mer 83507, France; email: sabine.charmasson@irsn.fr

[6]School of Nuclear Science and Engineering, Oregon State University, Corvallis, Oregon 97331; email: kathryn.higley@oregonstate.edu

[7]Institute of Mathematical Machine and System Problems, Kiev 03680, Ukraine; email: vladmad@gmail.com

[8]School of Science, Edith Cowan University, Joondalup 6027, Australia; email: p.masque@ecu.edu.au

[9]Departament de Física, Institut de Ciència i Tecnologia Ambientals, Universitat Autònoma de Barcelon, 08193 Bellaterra, Spain

[10]Environment Laboratories, International Atomic Energy Agency, MC 98000, Monaco; email: p.j.morris@iaea.org

[11]Centre for Environmental Radioactivity, Norwegian University of Life Sciences, Ås 1430, Norway; email: deborah.oughton@nmbu.no

[12]Bedford Institute of Oceanography, Dartmouth B2Y 4A2, Canada; email: john.smith@dfo-mpo.gc.ca

LITERATURE CITED

Aarkrog A, Baxter MS, Bettencourt AO, Bojanowski R, Bologa A, et al. 1997. A comparison of doses from ^{137}Cs and ^{210}Po in marine food: a major international study. *J. Environ. Radioact.* 34:69–90

Alam L, Mohamed CAR. 2011. Natural radionuclide of ^{210}Po in the edible seafood affected by coal-fired power plant industry in Kapar coastal area of Malaysia. *Environ. Health* 10:43

Aliyu AS, Ramli AT. 2015. The world's high background natural radiation areas (HBNRAs) revisited: a broad overview of the dosimetric, epidemiological and radiobiological issues. *Radiat. Meas.* 73:51–59

Ambe D, Kaeriyama H, Shigenobu Y, Fujimoto K, Ono T, et al. 2014. Five-minute resolved spatial distribution of radiocesium in sea sediment derived from the Fukushima Dai-Ichi nuclear power plant. *J. Environ. Radioact.* 138:264–75

Aoyama M, Fukasawa M, Hirose K, Hamajima Y, Kawano T, et al. 2011. Cross equator transport of ^{137}Cs from North Pacific Ocean to South Pacific Ocean (*BEAGLE2003* cruises). *Prog. Oceanogr.* 89:7–16

Aoyama M, Hamajima Y, Hult M, Uematsu M, Oka E, et al. 2016. ^{134}Cs and ^{137}Cs in the North Pacific Ocean derived from the March 2011 TEPCO Fukushima Dai-Ichi Nuclear Power Plant accident, Japan. Part one: surface pathway and vertical distributions. *J. Oceanogr.* 72:53–65

Aoyama M, Hirose K. 1995. The temporal and spatial variation of ^{137}Cs concentration in the Western North Pacific and its marginal seas during the period from 1979 to 1988. *J. Environ. Radioact.* 29:57–74

Aoyama M, Hirose K. 2004. Artificial radionuclides database in the Pacific Ocean: HAM database. *Sci. World J.* 4:200–15

Aoyama M, Hirose K, Nemoto K, Takatsuki Y, Tsumune D. 2008. Water masses labeled with global fallout ^{137}Cs formed by subduction in the North Pacific. *Geophys. Res. Lett.* 35:L01604

Bailly du Bois P, Laguionie P, Boust D, Korsakissok I, Didier D, Fiévet B. 2012. Estimation of marine source-term following Fukushima Dai-Ichi accident. *J. Environ. Radioact.* 114:2–9

Balonov MI, Anspaugh LR, Bouville A, Likhtarev IA. 2007. Contribution of internal exposures to the radiological consequences of the Chernobyl accident. *Radiat. Prot. Dosim.* 127:491–96

Behrens E, Schwarzkopf FU, Lübbecke JF, Böning CW. 2012. Model simulations on the long-term dispersal of ^{137}Cs released into the Pacific Ocean off Fukushima. *Environ. Res. Lett.* 7:034004

Belharet M, Estournel C, Charmasson S. 2016. Ecosystem model-based approach for modeling the dynamics of ^{137}Cs transfer to marine plankton populations: application to the Western North Pacific Ocean after the Fukushima nuclear power plant accident. *Biogeosciences* 13:499–516

Black E, Buesseler KO. 2014. Spatial variability and the fate of cesium in coastal sediments near Fukushima, Japan. *Biogeosciences* 11:7235–71

Bond NA, Cronin MF, Freeland H, Mantua N. 2015. Causes and impacts of the 2014 warm anomaly in the NE Pacific. *Geophys. Res. Lett.* 42:3414–20

Brenner DJ, Doll R, Goodhead DT, Hall EJ, Land CE, et al. 2003. Cancer risks attributable to low doses of ionizing radiation: assessing what we really know. *PNAS* 100:13761–66

Bu WT, Zheng J, Aono T, Tagami K, Uchida S, et al. 2013. Vertical distributions of plutonium isotopes in marine sediment cores off the Fukushima coast after the Fukushima Dai-ichi nuclear power plant accident. *Biogeosciences* 10:2497–511

Buesseler KO. 2012. Fishing for answers off Fukushima. *Science* 338:480–82

Buesseler KO. 2014. Fukushima and ocean radioactivity. *Oceanography* 27(1):92–105

Buesseler KO, Aoyama M, Fukasawa M. 2011. Impacts of the Fukushima nuclear power plants on marine radioactivity. *Environ. Sci. Technol.* 45:9931–35

Buesseler KO, German CR, Honda MC, Otosaka S, Black EE, et al. 2015. Tracking the fate of particle associated Fukushima Daiichi cesium in the ocean off Japan. *Environ. Sci. Technol.* 49:9807–16

Buesseler KO, Jayne SR, Fisher NS, Rypina II, Baumann H, et al. 2012. Fukushima-derived radionuclides in the ocean and biota off Japan. *PNAS* 109:5984–88

Buesseler KO, Livingston HD, Honjo S, Hay BJ, Konuk T, Kempe S. 1990. Scavenging and particle deposition in the southwestern black sea—evidence from Chernobyl radiotracers. *Deep-Sea Res. A* 37:413–30

Buesseler KO, Livingston HD, Honjo S, Hay BJ, Manganini SJ, et al. 1987. Chernobyl radionuclides in a Black Sea sediment trap. *Nature* 329:825–28

Calmet D, Charmassson S, Gontier G, Meisnez A, Boudouresque C-F. 1991. Chernobyl radionuclides in the Mediterranean seagrass *Posidonia oceanica*, 1986–1987. *J. Environ. Radioact.* 13:157–73

Cancer Netw. 1999. Total-body irradiation for bone marrow transplantation. *Oncology*, July 1. **http://www.cancernetwork.com/review-article/total-body-irradiation-bone-marrow-transplantation**

Carlson L, Holm E. 1992. Radioactivity in *Fucus vesiculosus* from the Baltic Sea following the Chernobyl accident. *J. Environ. Radioact.* 15:231–48

Casacuberta N, Masqué P, Garcia-Orellana J, Garcia-Tenorio R, Buesseler KO. 2013. ^{90}Sr and ^{89}Sr in seawater off Japan as a consequence of the Fukushima Dai-Ichi nuclear accident. *Biogeosciences* 10:2039–67

Castrillejo M, Casacuberta N, Breier CF, Pike SM, Masqué P, Buesseler KO. 2015. Reassessment of ^{90}Sr, ^{137}Cs, and ^{134}Cs in the coast off Japan derived from the Fukushima Dai-Ichi nuclear accident. *Environ. Sci. Technol.* 50:173–80

Charette MA, Breier CF, Henderson PB, Pike SM, Rypina II, et al. 2013. Radium-based estimates of cesium isotope transport and total direct ocean discharges from the Fukushima nuclear power plant accident. *Biogeosciences* 10:2159–67

Chartin C, Evrard O, Onda Y, Patin J, Lefèvre I, et al. 2013. Tracking the early dispersion of contaminated sediment along rivers draining the Fukushima radioactive pollution plume. *Anthropocene* 1:23–34

Chester A, Starosta K, Andreoiu C, Ashley R, Barton A, et al. 2013. Monitoring rainwater and seaweed reveals the presence of ^{131}I in southwest and central British Columbia, Canada following the Fukushima nuclear accident in Japan. *J. Environ. Radioact.* 124:205–13

Chino M, Nakayama H, Nagai H, Terada H, Katata G, Yamazawa H. 2011. Preliminary estimation of release amounts of ^{131}I and ^{137}Cs accidentally discharged from the Fukushima Daiichi nuclear power plant into the atmosphere. *J. Nucl. Sci. Technol.* 48:1129–34

Eckerman K, Harrison J, Menzel H, Clement C. 2013. ICRP publication 119: compendium of dose coefficients based on ICRP publication 60. *Ann. ICRP* 42:e1–130

Estournel C, Bosc E, Bocquet M, Ulses C, Marsaleix P, et al. 2012. Assessment of the amount of cesium-137 released into the Pacific Ocean after the Fukushima accident and analysis of its dispersion in Japanese coastal waters. *J. Geophys. Res.* 117:C11014

Evangeliou N, Balkanski Y, Cozic A, Møller AP. 2014. How "lucky" we are that the Fukushima disaster occurred in early spring: predictions on the contamination levels from various fission products released from the accident and updates on the risk assessment for solid and thyroid cancers. *Sci. Total Environ.* 500:155–72

Evrard O, Laceby JP, Lepage H, Onda Y, Cerdan O, Ayrault S. 2015. Radiocesium transfer from hillslopes to the Pacific Ocean after the Fukushima nuclear power plant accident: a review. *J. Environ. Radioact.* 148:92–110

FAJ (Fish. Agency Jpn.). 2015. *Report on the monitoring of radionuclides in fishery products (summary)*. Rep., Fish. Agency Jpn., Tokyo. **http://www.mofa.go.jp/files/000100400.pdf**

FAO (Food Agric. Organ. UN), WHO (World Health Organ.). 1994. *Codex Alimentarius*. Rome: FAO

Fisher NS, Beaugelin-Seiller K, Hinton TG, Baumann Z, Madigan DJ, Garnier-Laplace J. 2013. Evaluation of radiation doses and associated risk from the Fukushima nuclear accident to marine biota and human consumers of seafood. *PNAS* 110:10670–75

Fowler SW, Buat-Menard P, Yokoyama Y, Ballestra S, Holm E, Nguyen HV. 1987. Rapid removal of Chernobyl fallout from Mediterranean surface waters by biological activity. *Nature* 329:56–58

Fowler SW, Fisher NS. 2004. Radionuclides in the biosphere. In *Marine Radioactivity*, ed. HD Livingston, pp. 167–203. Oxford, UK: Elsevier

Fujimoto K, Miki S, Kaeriyama H, Shigenobu Y, Takagi K, et al. 2015. Use of otolith for detecting strontium-90 in fish from the harbor of Fukushima Dai-Ichi nuclear power plant. *Environ. Sci. Technol.* 49:7294–301

Fukushima Prefect. 2016a. *Fukushima revitalization*. Fukushima Prefect. Gov., Fukushima, Jpn. **http://www.pref.fukushima.lg.jp/site/portal-english/list385.html**

Fukushima Prefect. 2016b. *Steps for revitalization in Fukushima*. 17th ed. (July 27, 2016), Engl. Lang. Version, Fukushima Prefect. Gov., Fukushima, Jpn. **http://www.pref.fukushima.lg.jp.e.od.hp.transer.com/site/portal/ayumik-1.html**

Garnier-Laplace J, Beaugelin-Seiller K, Hinton TG. 2011. Fukushima wildlife dose reconstruction signals ecological consequences. *Environ. Sci. Technol.* 45:5077–78

Garnier-Laplace J, Gilbin R, eds. 2006. *Derivation of predicted no-effect-dose-rate values for ecosystems (and their sub-organisational levels) exposed to radioactive substances*. ERICA Deliv. D5, Eur. Comm., 6th Framew., Contract No. FI6R-CT-2003-508847

Guilderson TP, Tumey SJ, Brown TA, Buesseler KO. 2014. The 129-iodine content of subtropical Pacific waters: impact of Fukushima and other anthropogenic 129-iodine sources. *Biogeosciences* 11:4839–52

Hamada N, Ogino H, Fujimichi Y. 2012. Safety regulations of food and water implemented in the first year following the Fukushima nuclear accident. *J. Radiat. Res.* 53:641–71

Harada KH, Fujii Y, Adachi A, Tsukidate A, Asai F, Koizumi A. 2013. Dietary intake of radiocesium in adult residents in Fukushima Prefecture and neighboring regions after the Fukushima nuclear power plant accident: 24-h food-duplicate survey in December 2011. *Environ. Sci. Technol.* 47:2520–26

Harmelin-Vivien M, Bodiguel X, Charmasson S, Loizeau V, Mellon-Duval C, et al. 2012. Differential biomagnification of PCB, PBDE, Hg and radiocesium in the food web of the European hake from the NW Mediterranean. *Mar. Pollut. Bull.* 64:974–83

Hayata I, Kanda R, Minamihisamatsu M, Furukawa A, Sasaki MS. 2001. Cytogenetical dose estimation for 3 severely exposed patients in the JCO criticality accident in Tokai-mura. *J. Radiat. Res.* 42(Suppl.):S149–55

Heldal HE, Føyn L, Varskog P. 2003. Bioaccumulation of ^{137}Cs in pelagic food webs in the Norwegian and Barents Seas. *J. Environ. Radioact.* 65:177–85

Honda MC, Kawakami H. 2014. Sinking velocity of particulate radiocesium in the northwestern North Pacific. *Geophys. Res. Lett.* 41:3959–65

Honda MC, Kawakami H, Watanabe S, Saino T. 2013. Concentration and vertical flux of Fukushima-derived radiocesium in sinking particles from two sites in the northwestern Pacific Ocean. *Biogeosciences* 10:3525–34

Horiguchi T, Yoshii H, Mizuno S, Shiraishi H. 2016. Decline in intertidal biota after the 2011 great east Japan earthquake and tsunami and the Fukushima nuclear disaster: field observations. *Sci. Rep.* 6:20416

Huh C-A, Hsu S-C, Lin C-Y. 2012. Fukushima-derived fission nuclides monitored around Taiwan: free tropospheric versus boundary layer transport. *Earth Planet. Sci. Lett.* 319–20:9–14

IAEA (Int. At. Energy Agency). 2004. *Sediment Distribution Coefficients and Concentration Factors for Biota in the Marine Environment*. Vienna: IAEA

IAEA (Int. At. Energy Agency). 2015a. *The Fukushima Daiichi Accident*, Tech. Vol. 5: *Post-Accident Recovery*. Vienna: IAEA

IAEA (Int. At. Energy Agency). 2015b. *MARiS - Marine Information System*. Database, updated July 15. **http://maris.iaea.org**

ICRP (Int. Comm. Radiol. Prot.). 2007. ICRP publication 103: the 2007 recommendations of the International Commission on Radiological Protection. *Ann. ICRP* 37(2–4):1–332

Inomata Y, Aoyama M, Tsubono T, Tsumune D, Hirose K. 2016. Spatial and temporal distributions of ^{134}Cs and ^{137}Cs derived from the TEPCO Fukushima Daiichi nuclear power plant accident in the North Pacific Ocean by using optimal interpolation analysis. *Environ. Sci. Process. Impacts* 18:126–36

Inoue M, Kofuji H, Hamajima Y, Nagao S, Yoshida K, Yamamoto M. 2012. ^{134}Cs and ^{137}Cs activities in coastal seawater along northern Sanriku and Tsugaru Strait, northeastern Japan, after Fukushima Dai-Ichi nuclear power plant accident. *J. Environ. Radioact.* 111:116–19

Ito T, Otosaka S, Kawamura H. 2007. Estimation of total amounts of anthropogenic radionuclides in the Japan Sea. *J. Nucl. Sci. Technol.* 44:912–22

Iwata K, Tagami K, Uchida S. 2013. Ecological half-lives of radiocesium in 16 species in marine biota after the TEPCO's Fukushima Daiichi nuclear power plant accident. *Environ. Sci. Technol.* 47:7696–703

Johansen MP, Ruedig E, Tagami K, Uchida S, Higley K, Beresford NA. 2014. Radiological dose rates to marine fish from the Fukushima Daiichi accident: the first three years across the North Pacific. *Environ. Sci. Technol.* 49:1277–85

Kaeriyama H, Ambe D, Shigenobu Y, Fujimoto K, Ono T, et al. 2014. ^{134}Cs and ^{137}Cs in Seawater around Japan after the Fukushima Daiichi nuclear power plant accident. *Umi Kenkyu* 23:127–46

Kanda J. 2013. Continuing ^{137}Cs release to the sea from the Fukushima Dai-Ichi nuclear power plant through 2012. *Biogeosciences* 10:6107–13

Kasamatsu F. 1997. Natural variation of radionuclide ^{137}Cs concentration in marine organisms with special reference to the effect of food habits and trophic level. *Mar. Ecol. Prog. Ser.* 160:109–20

Katata G, Chino M, Kobayashi T, Terada H, Ota M, et al. 2015. Detailed source term estimation of the atmospheric release for the Fukushima Daiichi nuclear power station accident by coupling simulations of an atmospheric dispersion model with an improved deposition scheme and oceanic dispersion model. *Atmos. Chem. Phys.* 15:1029–70

Katata G, Ota M, Terada H, Chino M, Nagai H. 2012. Atmospheric discharge and dispersion of radionuclides during the Fukushima Dai-ichi nuclear power plant accident. Part I: source term estimation and local-scale atmospheric dispersion in early phase of the accident. *J. Environ. Radioact.* 109:103–13

Kawamura H, Kobayashi T, Furuno A, In T, Ishikawa Y, et al. 2011. Preliminary numerical experiments on oceanic dispersion of ^{131}I and ^{137}Cs discharged into the ocean because of the Fukushima Daiichi nuclear power plant disaster. *J. Nucl. Sci. Technol.* 48:1349–56

Kempe S, Nies H. 1986. Chernobyl nuclide record from a North Sea sediment trap. *Nature* 329:828–31

Kim Y, Cho S, Kang H-D, Kim W, Lee H-R, et al. 2006. Radiocesium reaction with illite and organic matter in marine sediment. *Mar. Pollut. Bull.* 52:659–65

Kobayashi T, Nagai H, Chino M, Kawamura H. 2013. Source term estimation of atmospheric release due to the Fukushima Dai-Ichi nuclear power plant accident by atmospheric and oceanic dispersion simulations. *J. Nucl. Sci. Technol.* 50:255–64

Kryshev I. 1995. Radioactive contamination of aquatic ecosystems following the Chernobyl accident. *J. Environ. Radioact.* 27:207–19

Kryshev I, Kryshev A, Sazykina T. 2012. Dynamics of radiation exposure to marine biota in the area of the Fukushima NPP in March-May 2011. *J. Environ. Radioact.* 114:157–61

Kryshev I, Sazykina T. 2011. Evaluation of the irradiation dose rate for marine biota in the region of the destroyed Fukushima reactor (Japan) in March-May 2011. *At. Energy* 111:55–60

Kumamoto Y, Aoyama M, Hamajima Y, Aono T, Kouketsu S, et al. 2014. Southward spreading of the Fukushima-derived radiocesium across the Kuroshio extension in the North Pacific. *Sci. Rep.* 4:4276

Kusakabe M, Ku TL, Harada K, Taguchi K, Tsunogai S. 1988. Chernobyl radioactivity found in mid-water sediment interceptors in the N. Pacific and Bering Sea. *Geophys. Res. Lett.* 15:44–47

Kusakabe M, Oikawa S, Takata H, Misonoo J. 2013. Spatiotemporal distributions of Fukushima-derived radionuclides in nearby marine surface sediments. *Biogeosciences* 10:5019–30

Landis JD, Hamm NT, Renshaw CE, Dade WB, Magilligan FJ, Gartner JD. 2012. Surficial redistribution of fallout ^{131}iodine in a small temperate catchment. *PNAS* 109:4064–69

Lawton CA. 1998. Total body irradiation for bone marrow transplantation. *Int. J. Radiat. Oncol. Biol. Phys.* 42(Suppl. 1):104

Little MP, Wakeford R, Bouville A, Simon SL. 2016. Measurement of Fukushima-related radioactive contamination in aquatic species. *PNAS* 113:3720–21

Livingston H, Anderson R. 1983. Large particle transport of plutonium and other fallout radionuclides to the deep ocean. *Nature* 303:228–31

Lujanienė G, Byčenkienė S, Povinec P, Gera M. 2012. Radionuclides from the Fukushima accident in the air over Lithuania: measurement and modelling approaches. *J. Environ. Radioact.* 114:71–80

Maderich V, Jung KT, Bezhenar R, de With G, Qiao F, et al. 2014. Dispersion and fate of ^{90}Sr in the Northwestern Pacific and adjacent seas: global fallout and the Fukushima Dai-ichi accident. *Sci. Total Environ.* 494–95:261–71

Madigan DJ, Baumann Z, Fisher NS. 2012. Pacific bluefin tuna transport Fukushima-derived radionuclides from Japan to California. *PNAS* 109:9483–86

MAFF (Minist. Agric. For. Fish.). 2015. *Results of the monitoring on radioactivity level in fisheries products*. **http://www.jfa.maff.go.jp/e/inspection/index.html**

Masson O, Baeza A, Bieringer J, Brudecki K, Bucci S, et al. 2011. Tracking of airborne radionuclides from the damaged Fukushima Dai-Ichi nuclear reactors by European networks. *Environ. Sci. Technol.* 45:7670–77

Mathews T, Fisher NS. 2008. Trophic transfer of seven trace metals in a four-step marine food chain. *Mar. Ecol. Prog. Ser.* 367:23–33

Mathieu A, Korsakissok I, Quélo D, Groëll J, Tombette M, et al. 2012. Atmospheric dispersion and deposition of radionuclides from the Fukushima Daiichi Nuclear power plant accident. *Elements* 8:195–200

Mettler FA Jr, Bhargavan M, Faulkner K, Gilley DB, Gray JE, et al. 2009. Radiologic and nuclear medicine studies in the United States and worldwide: frequency, radiation dose, and comparison with other radiation sources—1950–2007. *Radiology* 253:520–31

Mettler FA Jr, Huda W, Yoshizumi TT, Mahesh M. 2008. Effective doses in radiology and diagnostic nuclear medicine: a catalog. *Radiology* 248:254–63

Min B-I, Periáñez R, Kim I-G, Suh K-S. 2013. Marine dispersion assessment of ^{137}Cs released from the Fukushima nuclear accident. *Mar. Pollut. Bull.* 72:22–33

Mitchell PI, Condren OM, Vintró LL, McMahon CA. 1999. Trends in plutonium, americium and radiocaesium accumulation and long-term bioavailability in the western Irish Sea mud basin. *J. Environ. Radioact.* 44:223–51

Miyazawa Y, Masumoto Y, Varlamov S, Miyama T, Takigawa M, et al. 2013. Inverse estimation of source parameters of oceanic radioactivity dispersion models associated with the Fukushima accident. *Biogeosciences* 10:2349–63

Morino Y, Ohara T, Nishizawa M. 2011. Atmospheric behavior, deposition, and budget of radioactive materials from the Fukushima Daiichi nuclear power plant in March 2011. *Geophys. Res. Lett.* 38:L00G11

Nagao S, Kanamori M, Ochiai S, Tomihara S, Fukushi K, Yamamoto M. 2013. Export of ^{134}Cs and ^{137}Cs in the Fukushima river systems at heavy rains by Typhoon Roke in September 2011. *Biogeosciences* 10:6215–23

Nagaoka M, Yokoyama H, Fujita H, Nakano M, Watanabe H, Sumiya S. 2015. Spatial distribution of radionuclides in seabed sediments off Ibaraki coast after the Fukushima Daiichi nuclear power plant accident. *J. Radioanal. Nucl. Chem.* 303:1305–8

Natl. Cancer Inst. 2016. *Surveillance, Epidemiology, and End Results Program.* **http://seer.cancer.gov**

Nesterenko AV, Nesterenko VB, Yablokov AV. 2010. Chernobyl's radioactive contamination of food and people. *Ann. N.Y. Acad. Sci.* 1181:289–302

Neville DR, Phillips AJ, Brodeur RD, Higley KA. 2014. Trace levels of Fukushima disaster radionuclides in East Pacific albacore. *Environ. Sci. Technol.* 48:4739–43

Nishihara K, Yamagishi I, Yasuda K, Ishimori K, Tanaka K, et al. 2012. Radionuclide release to stagnant water in Fukushima-1 nuclear power plant. *Trans. At. Energy Soc. Jpn.* 11:13–19

Ogino H, Hattori T. 2014. Calculation of background lifetime risk of cancer mortality in Japan. *Jpn. J. Health Phys.* 49:194–98

Ohtsuru A, Tanigawa K, Kumagai A, Niwa O, Takamura N, et al. 2015. Nuclear disasters and health: lessons learned, challenges, proposals. *Lancet* 386:489–97

Oikawa S, Watabe T, Takata H, Misonoo J, Kusakabe M. 2015. Plutonium isotopes and ^{241}Am in surface sediments off the coast of the Japanese islands before and soon after the Fukushima Dai-Ichi nuclear power plant accident. *J. Radioanal. Nucl. Chem.* 303:1513–18

Okamura H, Ikeda S, Morita T, Eguchi S. 2016. Risk assessment of radioisotope contamination for aquatic living resources in and around Japan. *PNAS* 113:3838–43

Ono T, Ambe D, Kaeriyama H, Shigenobu Y, Fujimoto K, et al. 2015. Concentration of ^{134}Cs + ^{137}Cs bonded to the organic fraction of sediments offshore Fukushima, Japan. *Geochem. J.* 49:219–27

Otake M. 1996. Threshold for radiation-related severe mental retardation in prenatally exposed A-bomb survivors: a re-analysis. *Int. J. Radiat. Biol.* 70:755–63

Otosaka S, Kato Y. 2014. Radiocesium derived from the Fukushima Daiichi nuclear power plant accident in seabed sediments: initial deposition and inventories. *Environ. Sci. Process. Impacts* 16:978–90

Otosaka S, Kobayashi T. 2013. Sedimentation and remobilization of radiocesium in the coastal area of Ibaraki, 70 km south of the Fukushima Dai-Ichi nuclear power plant. *Environ. Monit. Assess.* 185:5419–33

Otosaka S, Nakanishi T, Suzuki T, Satoh Y, Narita H. 2014. Vertical and lateral transport of particulate radiocesium off Fukushima. *Environ. Sci. Technol.* 48:12595–602

Pentreath R, Allington D. 1988. Dose to man from the consumption of marine seafoods: a comparison of the naturally-occurring ^{210}Po with artificially-produced radionuclides. In *Proceedings of the Seventh International Congress of the International Radiation Protection Association*, pp. 1582–85. Washington, DC: Int. Radiat. Prot. Assoc.

Periáñez R, Suh K-S, Byung-Il M, Casacuberta N, Masqué P. 2013. Numerical modeling of the releases of ^{90}Sr from Fukushima to the ocean: an evaluation of the source term. *Environ. Sci. Technol.* 47:12305–13

Poole AJ, Denoon DC, Woodhead DS. 1997. The distribution and retention of ^{137}Cs in the subtidal sediments of the Irish Sea. *Radioprotection* 32:263–70

Pouil S, Warnau M, Oberhänsli F, Teyssié J-L, Metian M. 2015. Trophic transfer of ^{110m}Ag in the turbot *Scophthalmus maximus* through natural prey and compounded feed. *J. Environ. Radioact.* 150:189–94

Povinec PP, Hirose K. 2015. Fukushima radionuclides in the NW Pacific, and assessment of doses for Japanese and world population from ingestion of seafood. *Sci. Rep.* 5:9016

Povinec PP, Hirose K, Aoyama M. 2012. Radiostrontium in the western North Pacific: characteristics, behavior, and the Fukushima impact. *Environ. Sci. Technol.* 46:10356–63

Pratama MA, Yoneda M, Shimada Y, Matsui Y, Yamashiki Y. 2015. Future projection of radiocesium flux to the ocean from the largest river impacted by Fukushima Daiichi nuclear power plant. *Sci. Rep.* 5:8408

Pröhl G, Mück K, Likhtarev I, Kovgan L, Golikov V. 2002. Reconstruction of the ingestion doses received by the population evacuated from the settlements in the 30-km zone around the Chernobyl reactor. *Health Phys.* 82:173–81

Rossi V, Van Sebille E, Sen Gupta A, Garçon V, England MH. 2013. Multi-decadal projections of surface and interior pathways of the Fukushima cesium-137 radioactive plume. *Deep-Sea Res. I* 80:37–46

Rossi V, Van Sebille E, Sen Gupta A, Garçon V, England MH. 2014. Corrigendum to "Multi-decadal projections of surface and interior pathways of the Fukushima cesium-137 radioactive plume" [Deep-Sea Research I 80 (2013) 37–46]. *Deep-Sea Res. I* 82:72

Rypina II, Jayne SR, Yoshida S, Macdonald AM, Buesseler K. 2014. Drifter-based estimate of the 5 year dispersal of Fukushima-derived radionuclides. *J. Geophys. Res.* 119:8177–93

Rypina II, Jayne SR, Yoshida S, Macdonald AM, Douglass E, Buesseler K. 2013. Short-term dispersal of Fukushima-derived radionuclides off Japan: modeling efforts and model-data intercomparison. *Biogeosciences* 10:4973–90

Saunier O, Mathieu A, Didier D, Tombette M, Quélo D, et al. 2013. An inverse modeling method to assess the source term of the Fukushima nuclear power plant accident using gamma dose rate observations. *Atmos. Chem. Phys.* 13:11403–21

Schauer D. 2009. *Ionizing radiation exposure of the population of the United States*. Rep. 160, Natl. Counc. Radiat. Prot. Meas., Bethesda, MD

Shigenobu Y, Fujimoto K, Ambe D, Kaeriyama H, Ono T, et al. 2014. Radiocesium contamination of greenlings (*Hexagrammos Otakii*) off the coast of Fukushima. *Sci. Rep.* 4:6851

Sholkovitz E, Mann D. 1984. The pore water chemistry of ^{239,240}Pu and ^{137}Cs in sediments of Buzzards Bay, Massachusetts. *Geochim. Cosmochim. Acta* 48:1107–14

Smith JN, Brown RM, Williams WJ, Robert M, Nelson R, Moran SB. 2015. Arrival of the Fukushima radioactivity plume in North American continental waters. *PNAS* 112:1310–15

Sohtome T, Wada T, Mizuno T, Nemoto Y, Igarashi S, et al. 2014. Radiological impact of TEPCO's Fukushima Dai-Ichi nuclear power plant accident on invertebrates in the coastal benthic food web. *J. Environ. Radioact.* 138:106–15

Standring WJ, Dowdall M, Strand P. 2009. Overview of dose assessment developments and the health of riverside residents close to the "Mayak" PA facilities, Russia. *Int. J. Environ. Res. Public Health* 6:174–99

Staunton S, Roubaud M. 1997. Adsorption of ^{137}Cs on montmorillonite and illite: effect of charge compensating cation, ionic strength, concentration of Cs, K and fulvic acid. *Clays Clay Miner.* 45:251–60

Steinhauser G. 2014. Fukushima's forgotten radionuclides: a review of the understudied radioactive emissions. *Environ. Sci. Technol.* 48:4649–63

Steinhauser G, Brandl A, Johnson TE. 2014. Comparison of the Chernobyl and Fukushima nuclear accidents: a review of the environmental impacts. *Sci. Total Environ.* 470:800–17

Stohl A, Seibert P, Wotawa G, Arnold D, Burkhart J, et al. 2012. Xenon-133 and caesium-137 releases into the atmosphere from the Fukushima Dai-Ichi nuclear power plant: determination of the source term, atmospheric dispersion, and deposition. *Atmos. Chem. Phys.* 12:2313–43

Tagami K, Uchida S. 2016. Consideration on the long ecological half-life component of ^{137}Cs in demersal fish based on field observation results obtained after the Fukushima accident. *Environ. Sci. Technol.* 50:1804–11

Tanaka K, Shimada A, Hoshi A, Yasuda M, Ozawa M, Kameo Y. 2014. Radiochemical analysis of rubble and trees collected from Fukushima Daiichi nuclear power station. *J. Nucl. Sci. Technol.* 51:1032–43

Tanigawa K, Hosoi Y, Hirohashi N, Iwasaki Y, Kamiya K. 2012. Loss of life after evacuation: lessons learned from the Fukushima accident. *Lancet* 379:889–91

Tateda Y, Tsumune D, Tsubono T. 2013. Simulation of radioactive cesium transfer in the southern Fukushima coastal biota using a dynamic food chain transfer model. *J. Environ. Radioact.* 124:1–12

Tateda Y, Tsumune D, Tsubono T, Aono T, Kanda J, Ishimaru T. 2015. Radiocesium biokinetics in olive flounder inhabiting the Fukushima accident-affected Pacific coastal waters of eastern Japan. *J. Environ. Radioact.* 147:130–41

TEPCO (Tokyo Electr. Power Co.). 2016. *Analysis results of fish and shellfish (the ocean area within 20km radius of Fukushima Daiichi NPS)*. **http://www.tepco.co.jp/en/nu/fukushima-np/f1/smp/index-e.html**

Terada H, Katata G, Chino M, Nagai H. 2012. Atmospheric discharge and dispersion of radionuclides during the Fukushima Dai-Ichi nuclear power plant accident. Part I: verification of the source term and analysis of regional-scale atmospheric dispersion. *J. Environ. Radioact.* 112:141–54

Thorne MC. 2003. Background radiation: natural and man-made. *J. Radiol. Prot.* 23:29–42

Thornton B, Ohnishi S, Ura T, Odano N, Sasaki S, et al. 2013. Distribution of local ^{137}Cs anomalies on the seafloor near the Fukushima Dai-Ichi nuclear power plant. *Mar. Pollut. Bull.* 74:344–50

Tsubono T, Misumi K, Tsumune D, Bryan FO, Hirose K, Aoyama M. 2016. Evaluation of radioactive cesium impact from atmospheric deposition and direct release fluxes into the North Pacific from the Fukushima Daiichi nuclear power plant. *Deep-Sea Res. I.* 115:10–21

Tsumune D, Tsubono T, Aoyama M, Hirose K. 2012. Distribution of oceanic ^{137}Cs from the Fukushima Daiichi nuclear power plant simulated numerically by a regional ocean model. *J. Environ. Radioact.* 111:100–8

Tsumune D, Tsubono T, Aoyama M, Uematsu M, Misumi K, et al. 2013. One-year, regional-scale simulation of ^{137}Cs radioactivity in the ocean following the Fukushima Daiichi nuclear power plant accident. *Biogeosciences* 10:5601–17

UNSCEAR (UN Sci. Comm. Effects At. Radiat.). 2000. *Sources and effects of ionizing radiation, Annex J: exposures and effects of the Chernobyl accident*. Rep., UN, New York

UNSCEAR (UN Sci. Comm. Effects At. Radiat.). 2008. *Sources and effects of ionizing radiation, Volume 1: UNSCEAR 2008 report to the general assembly with scientific annexes*. Rep. A/63/46, UN, New York

UNSCEAR (UN Sci. Comm. Effects At. Radiat.). 2014. *Sources, effects and risks of ionizing radiation, Volume 1: UNSCEAR 2013 report to the general assembly and scientific annex A*. Rep. A/68/46, UN, New York

Vives i Batlle J, Aono T, Brown JE, Hosseini A, Garnier-Laplace J, et al. 2014. The impact of the Fukushima nuclear accident on marine biota: retrospective assessment of the first year and perspectives. *Sci. Total Environ.* 487:143–53

Wada T, Nemoto Y, Shimamura S, Fujita T, Mizuno T, et al. 2013. Effects of the nuclear disaster on marine products in Fukushima. *J. Environ. Radioact.* 124:246–54

WHO (World Health Organ.). 2013. *Health risk assessment from the nuclear accident after the 2011 Great East Japan earthquake and tsunami, based on a preliminary dose estimation*. Rep., WHO, Geneva

Winiarek V, Bocquet M, Duhanyan N, Roustan Y, Saunier O, Mathieu A. 2014. Estimation of the caesium-137 source term from the Fukushima Daiichi nuclear power plant using a consistent joint assimilation of air concentration and deposition observations. *Atmos. Environ.* 82:268–79

Wu J, Zheng J, Dai M, Huh C-A, Chen W, et al. 2014. Isotopic composition and distribution of plutonium in northern South China Sea sediments revealed continuous release and transport of Pu from the Marshall Islands. *Environ. Sci. Technol.* 48:3136–44

Yamada M, Aono T, Hirano S. 1999. $^{239+240}$Pu and ^{137}Cs concentrations in fish, cephalopods, crustaceans, shellfish, and algae collected around the Japanese coast in the early 1990s. *Sci. Total Environ.* 239:131–42

Yamashiki Y, Onda Y, Smith HG, Blake WH, Wakahara T, et al. 2014. Initial flux of sediment-associated radiocesium to the ocean from the largest river impacted by Fukushima Daiichi nuclear power plant. *Sci. Rep.* 4:3714

Yoshida S, Macdonald AM, Jayne SR, Rypina II, Buesseler KO. 2015. Observed eastward progression of the Fukushima ^{134}Cs signal across the North Pacific. *Geophys. Res. Lett.* 42:7139–47

Zhao X, Wang W-X, Yu K, Lam PK. 2001. Biomagnification of radiocesium in a marine piscivorous fish. *Mar. Ecol. Prog. Ser.* 222:227–37

Zheng J, Aono T, Uchida S, Zhang J, Honda MC. 2012. Distribution of Pu isotopes in marine sediments in the Pacific 30 km off Fukushima after the Fukushima Daiichi nuclear power plant accident. *Geochem. J.* 46:361–69

Zheng J, Tagami K, Uchida S. 2013. Release of plutonium isotopes into the environment from the Fukushima Daiichi nuclear power plant accident: what is known and what needs to be known. *Environ. Sci. Technol.* 47:9584–95